WESTINGHOUSE CLASS 3
CUSTOMER DESIGNATED DISTRIBUTION

WCAP-11726

ANALYSIS OF CAPSULE V FROM THE SOUTH CAROLINA ELECTRIC AND GAS COMPANY VIRGIL C. SUMMER UNIT 1 REACTOR VESSEL RADIATION SURVEILLANCE PROGRAM

D. J. Colburn
L. A. Lamantia
L. Albertin

January 1988

APPROVED: T. A. Meyer

T. A. Meyer, Manager
Structural Materials and Reliability Technology

Work performed under Shop Order No. CFZJ-106

Prepared by Westinghouse Electric Corporation for the South Carolina Electric and Gas Company

WESTINGHOUSE ELECTRIC CORPORATION
Nuclear Energy Systems
P. O. Box 2728
Pittsburgh, Pennsylvania 15230

PREFACE

This report has been technically reviewed and verified.

	Reviewer	
Sections 1 through 5 and 7	S. E. Yanichko	S E Yanichko
Section 6	S. L. Anderson	S L Anderson for SLA

CONTENTS

LIST OF ILLUSTRATIONS

LIST OF TABLES

1. SUMMARY OF RESULTS

The analysis of the reactor vessel material contained in surveillance Capsule V, the second capsule to be removed from the V. C. Summer Unit 1 pressure vessel, led to the following conclusions:

- The capsule received an average fast neutron fluence ($E > 1$ MeV) of 1.47×10^{19} n/cm^2.
- Irradiation of the reactor vessel intermediate shell plate A9154-1 to 1.47×10^{19} n/cm^2 resulted in 30 and 50 ft-lb transition temperature increases of 60°F and 65°F, respectively, for specimens oriented parallel to the major working direction (longitudinal orientation) and increases of 40°F and 55°F, respectively for specimens oriented normal to the major working direction (transverse orientation).
- Weld metal irradiated to 1.47×10^{19} n/cm^2 resulted in both a 30 and 50 ft-lb transition temperature increase of 45°F.
- The average upper shelf energy (transverse orientation) of the plate A9154-1 increased from 75 to 76 ft-lb, and the limiting weld decreased from 91 to 85 ft-lb after irradiation to 1.47×10^{19} n/cm^2. Both materials exhibit a more than adequate upper shelf energy level for continued safe plant operation and are expected to maintain an upper shelf energy of no less than 50 ft-lb throughout the life of the vessel as required by 10CFR50, Appendix G.
- The surveillance capsule test results do not indicate any significant changes in the RT_{NDT} values projected for the reactor vessel, and, therefore, a low risk of vessel failure from pressurized thermal shock (PTS) events is postulated.

2. INTRODUCTION

This report presents the results of the examination of Capsule V, the second capsule to be removed from the reactor in the continuing surveillance program which monitors the effects of neutron irradiation on the V. C. Summer Unit 1 reactor pressure vessel materials under actual operating conditions.

The surveillance program for the V. C. Summer Unit 1 reactor pressure vessel materials was designed and recommended by the Westinghouse Electric Corporation. A description of the surveillance program and the preirradiation mechanical properties of the reactor vessel materials are presented by Davidson and Yanichko.[1] The surveillance program was planned to cover the 40-year design life of the reactor pressure vessel and was based on ASTM E-185-79, "Standard Practice for Conducting Surveillance Tests for Light Water Nuclear Power Reactor Vessels". Westinghouse Nuclear Energy Systems personnel were contracted for the preparation of procedures for removing the capsule from the reactor and its shipment to the Westinghouse Research and Development Center where the postirradiation mechanical testing of the Charpy V-notch impact and tensile surveillance specimens were performed.

This report summarized the testing of and the postirradiation data obtained from surveillance Capsule V removed from the V. C. Summer Unit 1 reactor vessel and discusses the analysis of these data.

3. BACKGROUND

The ability of the large steel pressure vessel containing the reactor core and its primary coolant to resist fracture constitutes an important factor in ensuring safety in the nuclear industry. The beltline region of the reactor pressure vessel is the most critical region of the vessel because it is subjected to significant fast neutron bombardment. The overall effects of fast neutron irradiation on the mechanical properties of low alloy, ferritic pressure vessel steels such as SA 533 Grade B Class 1 (base material of the V. C. Summer Unit 1 reactor pressure vessel beltline) are well documented in the literature. Generally, low alloy ferritic materials show an increase in hardness and tensile properties and a decrease in ductility and toughness under certain conditions of irradiation.

A method for performing analyses to guard against fast fracture in reactor pressure vessels have been presented in "Protection Against Nonductile Failure", Appendix G to Section III of the ASME Boiler and Pressure Vessel Code. The method uses fracture mechanics concepts and is based on the reference nil-ductility temperature (RT_{NDT}).

RT_{NDT} is defined as the greater of either the drop weight nil-ductility transition temperature (NDTT per ASTM E-208) or the temperature 60°F less than the 50 ft-lb (and 35-mil lateral expansion) temperature as determined from Charpy specimens oriented normal (transverse) to the major working direction of the material. The RT_{NDT} of a given material is used to index that material to a reference stress intensity factor curve (K_{IR} curve) which appears in Appendix G of the ASME Code. The K_{IR} curve is a lower bound of dynamics, crack arrest, and static fracture toughness results obtained from several heats of pressure vessel steel. When a given material is indexed to the K_{IR} curve, allowable stress intensity factors can be obtained for this

material as a function of temperature. Allowable operating limits can then be determined using these allowable stress intensity factors.

RT_{NDT} and, in turn, the operating limits of nuclear power plants can be adjusted to account for the effects of radiation on the reactor vessel material properties. The radiation embrittlement changes in mechanical properties of a given reactor pressure vessel steel can be monitored by a reactor surveillance program such as the V. C. Summer Unit 1 Reactor Vessel Radiation Surveillance Program,[1] in which a surveillance capsule is periodically removed from the operating nuclear reactor and the encapsulated specimens are tested. The increase in the average Charpy V-notch 30 ft-lb temperature (ΔRT_{NDT}) due to irradiation is added to the original RT_{NDT} to adjust the RT_{NDT} for radiation embrittlement. This adjusted RT_{NDT} (RT_{NDT} initial + ΔRT_{NDT}) is used to index the material to the K_{IR} curve and, in turn, to set operating limits for the nuclear power plant which take into account the effects of irradiation on the reactor vessel materials. The unirradiated vessel material data for V. C. Summer Unit 1 is shown in Table 3-1.

Table 3-1. V. C. Summer Unit 1 Reactor Vessel Toughness Data (Unirradiated)

Component	Heat No.	Grade	Cu %	P %	Ni %	NDT °F	50 ft-lb 35 mil Temp °F	RT_{NDT} °F	MWD[a] Shelf Energy ft-lbs	NMWD[b] Shelf Energy ft-lbs
Closure Dome	A9231-1	A533B Cl. 1	-	.009	.46	-20	40	-20	-	106.0
Head Flange	5297-V1	A508 Cl. 2	-	.009	.70	10	<60	10	-	129.0
Vessel Flange	5301-V1	" "	-	.007	.70	0	<60	0	-	172.0
Inlet Nozzle	436B-1	" "	-	.005	.76	-20	<40	-20	-	130.0
" "	436B-2	" "	-	.005	.81	0	<60	0	-	114.5
" "	436B-3	" "	-	.005	.81	-20	<40	-20	-	135.0
Outlet Nozzle	437B-1	" "	-	.007	.81	-10	<50	-10	-	146.0
" "	437B-2	" "	-	.006	.80	-10	<50	-10	-	165.0
" "	437B-3	" "	-	.006	.78	0	<50	0	-	150.0
Nozzle Shell	C9955-2	A533B Cl. 1	.13	.010	.57	-20	78	18	-	100.5
" "	C0123-2	" "	.12	.009	.58	-30	86	26	-	91.0
Inter. Shell	A9154-1	" "	.10	.009	.51	-20	90	30	136	80.5
" "	A9153-2	" "	.09	.006	.45	-20	40	-20	141	106.5
Lower Shell	C9923-2	" "	.08	.005	.41	-10	70	10	161	91.5
" "	C9923-1	" "	.08	.005	.41	-30	70	10	148	106.0
Bottom Hd. Ring	A9249-1	" "	-	.010	.53	-40	23	-37	-	107.0
Bottom Dome	A9231-2	" "	-	.010	.45	-10	42	-10	-	134.0
Inter. to Lower Shell Girth Weld			.06	.013	.89	-50	16	-44	-	84.0
Inter. & Lower Shell Long. Welds			.06	.013	.89	-50	16	-44	-	84.0
Weld HAZ			-	-	-	-70	-37	-70	-	130.0

[a] Major Working Direction

[b] Normal to Major Working Direction

4. DESCRIPTION OF PROGRAM

Six surveillance capsules for monitoring the effects of neutron exposure on the V. C. Summer Unit 1 reactor pressure vessel core region material were inserted in the reactor vessel prior to initial plant startup. The six capsules were positioned in the reactor vessel between the neutron shielding pads and the vessel wall as shown in Figure 4-1. The vertical center of the capsules is opposite the vertical center of the core.

Capsule V was removed after 2.93 effective full power years of plant operation. This capsule contained Charpy V-notch, tensile, and 1/2 T compact tension (CT) specimens (Figure 4-2) from the intermediate shell plate A9154-1 and submerged arc weld metal representative of the intermediate to lower shell beltline weld seam of the reactor vessel and Charpy V-notch specimens from weld heat-affected zone (HAZ) material. All heat-affected zone specimens were obtained from within the HAZ of plate A9154-1 of the representative weld.

The chemistry and heat treatment data from the V. C. Summer Unit 1 surveillance material are presented in Tables 4-1 and 4-2, respectively.

All test specimens were machined from the 1/4 thickness location of the plate. Test specimens represent material taken at least one plate thickness from the quenched end of the plate. Base metal Charpy V-notch impact and tension specimens were oriented with the longitudinal axis of the specimen parallel to the major working direction of the plate (longitudinal orientation) and also normal to the major working direction (transverse orientation). Charpy V-notch and tensile specimens from the weld metal were oriented with the longitudinal axis of the specimens transverse to the welding direction. The CT specimens in Capsule V were machined such that the simulated crack in the specimen would propagate normal and parallel to the major working direction for the plate specimen and parallel to the weld direction.

Capsule V contained dosimeter wires of pure copper, iron, nickel, and aluminum-0.15% cobalt (cadmium-shielded and unshielded). In addition, cadmium shielded dosimeters of neptunium (Np^{237}) and uranium (U^{238}) were contained in the capsule.

Thermal monitors made from the two low-melting eutectic alloys and sealed in Pyrex tubes were included in the capsule. The composition of the two alloys and their melting points are as follows.

2.5% Ag, 97.5% Pb	Melting Point: 579°F (304°C)
1.75% Ag, 0.75% Sn, 97.5% Pb	Melting Point: 590°F (310°C)

The arrangement of the various mechanical specimens, dosimeters and thermal monitors contained in Capsule V are shown in Figure 4-2.

Table 4-1

Chemical Composition of the V. C. Summer Unit 1
Reactor Vessel Surveillance Materials

Element	Plate A9154-1 Lukens Steel Co. Analysis	Weld Metal[c] Lukens Steel Co. Analysis
C	0.22	0.085
S	0.015	0.012/0.007[b]
N_2	0.0076	0.015
Co	0.010	0.060/0.01[b]
Cu	0.10	0.05/0.04[b]
Si	0.24	0.48/0.42[b]
Mo	0.49	0.49/0.46[b]
Ni	0.51	0.91/0.95[b]
Mn	1.30	1.32/1.50[b]
Cr	0.08	0.14/0.12[b]
V	0.001[a]	0.005
P	0.009	0.013/0.009[b]
Sn	0.007	0.0047
Al	0.024	0.007/0.03[b]
B	0.0004	0.0005
Ti	0.0002	0.001
Pb	<0.005	0.0206
Zr	0.001	0.001
As	0.006	0.006
W	<0.01	0.01

[a] Westinghouse Analysis.

[b] Analysis performed on irradiated weld specimen CW14.

[c] Surveillance weld was made of the same RACO INMM wire Heat #4P4784 and Linde 124 Flux Lot No. 3930 as the beltline welds of the reactor vessel.

Table 4-2

Heat Treatment of the V. C. Summer Unit 1
Reactor Vessel Surveillance Materials

Material	Temperature (°F)	Time(Hr)	Coolant
Shell Plate A9154-1	1550°/1650°	1/2 hr/in., min.	Water quenched
	1225° ±25°	1/2 hr/in., min.	Air cooled
	1150° ±25°	43	Furnace cooled to 600°F
Weldment	1150° ± 25°	12	Furnace cooled

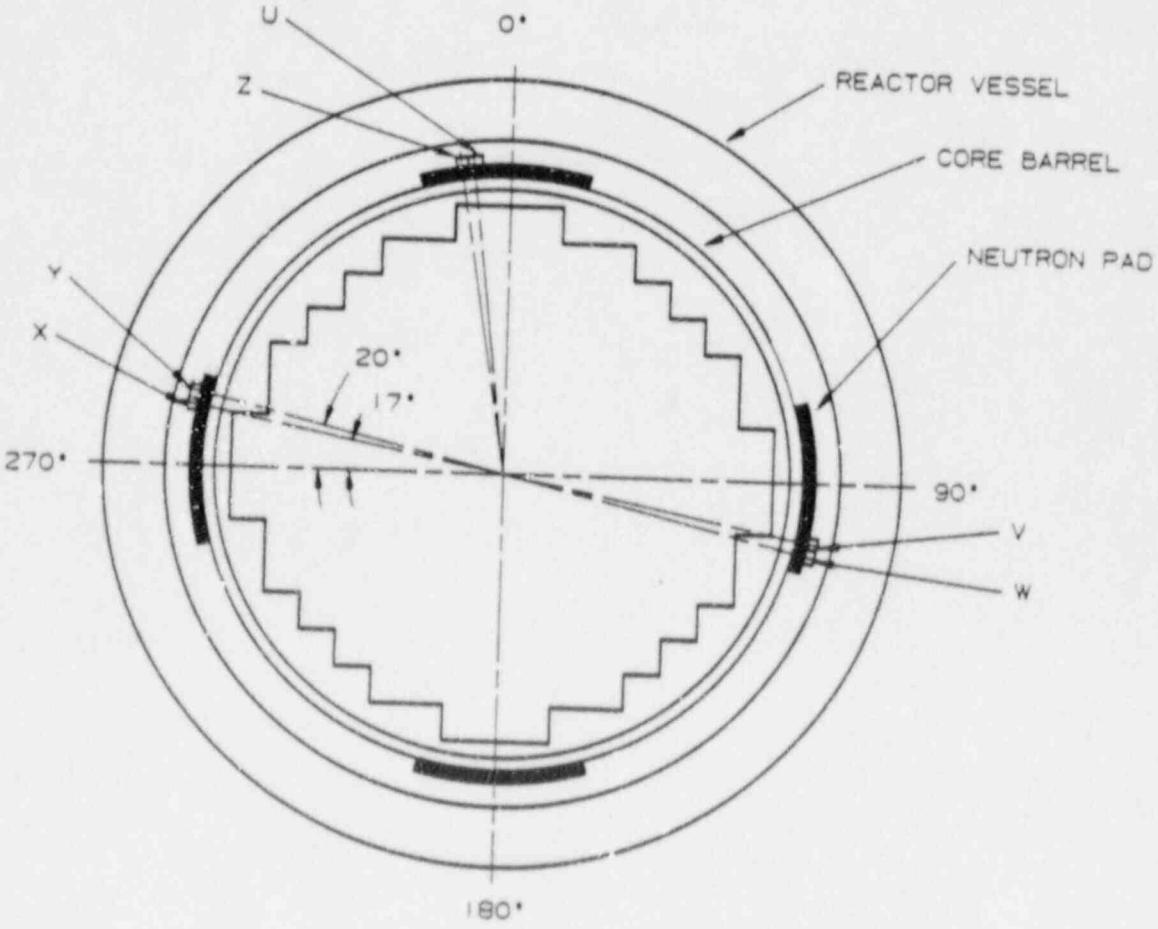

Figure 4-1. Arrangement of surveillance capsules in the V. C. Summer Unit 1 reactor vessel

SPECIMEN NUMBERING CODE:

CT - PLATE A9154-1 (TRANSVERSE ORIENTATION)
CL - PLATE A9154-1 (LONGITUDINAL ORIENTATION)
CW - CORE REGION WELD METAL
CH - HEAT-AFFECTED-ZONE METAL

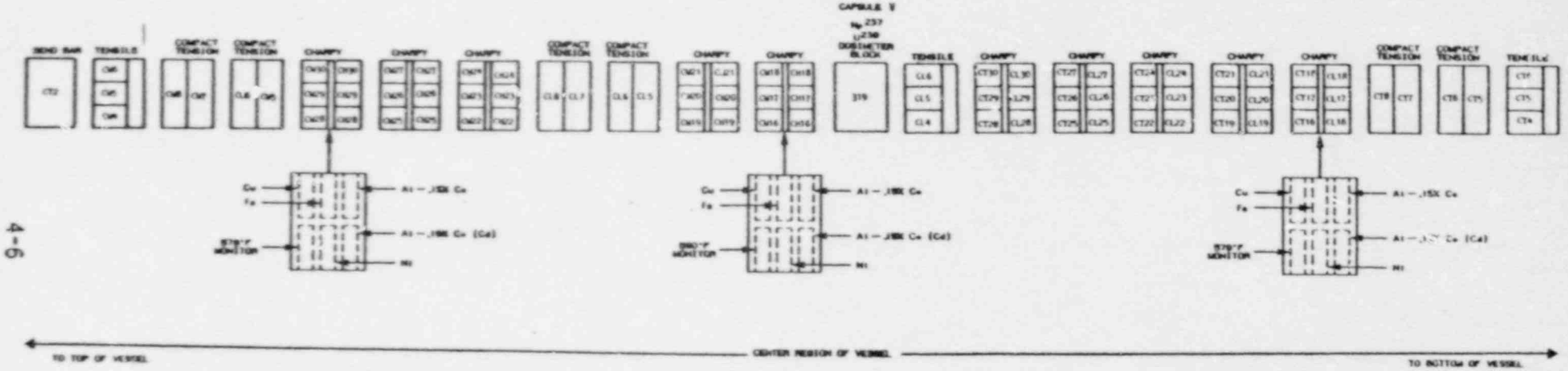

Figure 4-2.
Capsule V Diagram Showing Location of Specimens, Thermal Monitors, and Dosimeters

5. TESTING OF SPECIMENS FROM CAPSULE V

5.1 OVERVIEW

The post-irradiation mechanical testing of the Charpy V-notch and tensile specimens was performed at the Westinghouse Research and Development Center with consultation by Westinghouse Nuclear Energy Systems personnel. Testing was performed in accordance with 10CFR50, Appendices G and H,[2] ASTM Specification E185-82, and Westinghouse Procedure RMF-8402, Revision 0 as modified by RMF Procedures 8102 and 8103.

Upon receipt of the capsule at the laboratory, the specimens and spacer blocks were carefully removed, inspected for identification number, and checked against the master list in WCAP-9234.[1] No discrepancies were found.

Examination of the two low-melting point 304°C (579°F) and 310°C (590°F) eutectic alloys indicated no melting of either type of thermal monitor. Based on this examination, the maximum temperature to which the test specimens were exposed was less than 304°C (579°F).

The Charpy impact tests were performed per ASTM Specification E23-82 and RMF Procedure 8103 on a Tinius-Olsen Model 74,358J machine. The tup (striker) of the Charpy machine is instrumented with an Effects Technology Model 500 instrumentation system. With this system, load-time and energy-time signals can be recorded in addition to the standard measurement of Charpy energy (E_D). From the load-time curve, the load of general yielding (P_{GY}), the time to general yielding (t_{GY}), the maximum load (P_M), and the time to maximum load (t_M) can be determined. Under some test conditions, a sharp drop in load indicative of fast fracture was observed. The load at which fast fracture was initiated is identified as the fast fracture load (P_F), and the load at which fast fracture terminated is identified as the arrest load (P_A).

The energy at maximum load (E_M) was determined by comparing the energy-time record and the load-time record. The energy at maximum load is roughly equivalent to the energy required to initiate a crack in the specimen. Therefore, the propagation energy for the crack (E_p) is the difference between the total energy to fracture (E_D) and the energy at maximum load.

The yield stress (σ_Y) is calculated from the three-point bend formula. The flow stress is calculated from the average of the yield and maximum loads, also using the three-point bend formula.

Percent shear was determined from post-fracture photographs using the ratio-of-areas methods in compliance with ASTM Specification A370-77. The lateral expansion was measured using a dial gage rig similar to that shown in the same specification.

Tension tests were performed on a 20,000-pound Instron, split-console test machine (Model 1115) per ASTM Specification E8-83 and E21-79, and RMF Procedure 8102. All pull rods, grips, and pins were made of Inconel 718 hardened to Rc 45. The upper pull rod was connected through a universal joint to improve axiality of loading. The tests were conducted at a constant crosshead speed of 0.05 inches per minute throughout the test.

Deflection measurements were made with a linear variable displacement transducer (LVDT) extensometer. The extensometer knife edges were spring-loaded to the specimen and operated through specimen failure. The extensometer gage length is 1.00 inch. The extensometer is rated as Class B-2 per ASTM E83-67.

Elevated test temperatures were obtained with a three-zone electric resistance split-tube furnace with a 9-inch hot zone. All tests were conducted in air.

Because of the difficulty in remotely attaching a thermocouple directly to the specimen, the following procedure was used to monitor specimen temperature. Chromel-alumel thermocouples were inserted in shallow holes in the center and each end of the gage section of a dummy

specimen and in each grip. In the test configuration, with a slight load on the specimen, a plot of specimen temperature versus upper and lower grip and controller temperatures was developed over the range of room temperature to 550°F (288°C). The upper grip was used to control the furnace temperature. During the actual testing the grip temperatures were used to obtain desired specimen temperatures. Experiments indicated that this method is accurate to ±2°F.

The yield load, ultimate load, fracture load, total elongation, and uniform elongation were determined directly from the load-extension curve. The yield strength, ultimate strength, and fracture strength were calculated using the original cross-sectional area. The final diameter and final gage length were determined from post-fracture photographs. The fracture area used to calculate the fracture stress (true stress at fracture) and percent reduction in area was computed using the final diameter measurement.

5.2 CHARPY V-NOTCH IMPACT TEST RESULTS

The results of Charpy V-notch impact tests performed on the various materials contained in Capsule V irradiated at 1.47×10^{19} n/cm^2 are presented in Tables 5-1 through 5-4 and Figures 5-1 through 5-4. The transition temperature increases and upper shelf energy decreases for the Capsule V materials are summarized in Table 5-5.

Irradiation of vessel intermediate shell plate A9154-1 material (longitudinal orientation) specimens to 1.47×10^{19} n/cm^2 (Figure 5-1) resulted in a 60°F and 65°F increase in 30 and 50 ft-lb transition temperatures respectively, and an upper shelf energy decrease of 10 ft-lb.

Irradiation of vessel intermediate sh... p... A9154-1 material (transverse orientation) specimens to 1.47×10^{19} n/cm^2 (Figure 5-2) resulted in 30 and 50 ft-lb transition temperature increases of 40°F and 55°F, respectively. The irradiated upper shelf energy experienced an increase of 1 ft-lb when compared to the unirradiated data.

Weld metal irradiated to 1.47 x 10^{19} n/cm^2 (Figure 5-3) resulted in both 30 and 50 ft-lb transition temperature increases of 45°F and an upper shelf energy decrease of 6 ft-lb.

Weld HAZ metal irradiated to 1.47 x 10^{19} n/cm^2 (Figure 5-4) resulted in 30 and 50 ft-lb transition temperature increases of 45°F and 55°F, respectively, and an upper shelf energy decrease of 19 ft-lb.

The fracture appearance of each irradiated Charpy specimen from the various materials is shown in Figures 5-5 through 5-8 and show an increasingly ductile or tougher appearance with increasing test temperature.

A comparison of the 30 ft-lb transition temperature increases for the various V. C. Summer Unit 1 surveillance materials with predicted increases using the methods of NRC Regulatory Guide 1.99, Revision 2[3] is presented in Table 5-6. This comparison indicates that the transition temperature increases resulting from irradiation to 1.47 x 10^{19} n/cm^2 are conservative compared to the Guide predictions.

5.3 TENSION TEST RESULTS

The results of tension tests performed on plate A9154-1 (longitudinal and transverse orientation) and the weld metal irradiated to 1.47 x 10^{19} n/cm^2 are shown in Table 5-7 and Figures 5-9, 5-10 and 5-11. Plate A9154-1 test results are shown in Figures 5-9 and 5-10 and indicate that irradiation to 1.47 x 10^{19} n/cm^2 caused a less than 10 ksi increase in the 0.2 percent offset yield strength and ultimate tensile strength. Weld metal tension test results shown in Figure 5-11, show that the ultimate tensile strength and the 0.2 percent offset yield strength increased by approximately 5 ksi with irradiation. The fractured tension specimens for the plate material are shown in Figures 5-12 and 5-13, while the fractured specimens for the weld metal are shown in Figure 5-14. A typical stress-strain curve for the tension tests is shown in Figure 5-15.

5.4 COMPACT TENSION TESTS

Per the surveillance capsule testing contract with South Carolina Electric and Gas, 1/2 T-compact tension (CT) specimens will not be tested. CT specimen will be stored at the Hot Cell at the Westinghouse R&D Center.

Table 5-1

Charpy V-Notch Impact Data for the V. C. Summer Unit 1
Shell Plate A9154-1 Irradiated at 550°F,
Fluence 1.47 x 10^{19} n/cm^2 (E > 1.0 MeV)

Sample No.	Temperature (°F)	(°C)	Impact Energy (ft-lb)	(J)	Lateral Expansion (mils)	(mm)	Shear (%)
			Longitudinal Orientation				
CL19	0	(-18)	6.0	(8.0)	6.0	(0.15)	2
CC30	25	(- 4)	24.0	(32.5)	24.0	(0.61)	10
CL28	25	(- 4)	32.0	(43.5)	25.5	(0.65)	15
CL20	50	(10)	38.0	(51.5)	34.5	(0.88)	15
CL22	50	(10)	44.0	(59.5)	34.5	(0.88)	20
CL29	77	(25)	73.0	(99.0)	52.5	(1.33)	45
CL26	78	(26)	79.0	(107.0)	53.0	(1.35)	50
CL21	100	(38)	23.0	(31.0)	22.5	(0.57)	20
CL16	100	(38)	70.0	(95.0)	51.5	(1.31)	50
CL18	125	(52)	65.0	(88.0)	49.0	(1.24)	50
CL24	150	(66)	100.0	(135.5)	79.5	(2.02)	90
CL23	200	(93)	125.0	(169.5)	83.5	(2.11)	95
CL17	250	(121)	121.0	(164.0)	82.5	(2.10)	100
CL25	350	(177)	119.0	(161.5)	85.5	(2.17)	100
CL27	400	(204)	125.0	(169.5)	80.5	(2.04)	100
			Transverse Orientation				
CT21	-50	(-46)	5.0	(7.0)	5.0	(0.13)	2
CT19	0	(-18)	14.0	(19.0)	13.0	(0.33)	5
CT24	50	(10)	25.0	(34.0)	26.0	(0.66)	15
CT18	50	(10)	44.0	(59.5)	25.0	(0.64)	20
CT16	77	(25)	35.0	(47.5)	32.0	(0.81)	20
CT30	78	(26)	33.0	(44.5)	28.0	(0.71)	20
CT20	100	(38)	40.0	(54.0)	41.0	(1.04)	35
CT28	100	(38)	44.0	(60.0)	34.5	(0.88)	35
CT22	125	(52)	34.0	(46.0)	36.5	(0.93)	30
CT27	125	(52)	46.0	(62.5)	42.5	(1.08)	35
CT17	150	(66)	52.0	(70.5)	49.5	(1.26)	45
CT26	250	(121)	77.0	(104.5)	62.5	(1.59)	100
CT29	300	(149)	73.0	(99.0)	71.0	(1.80)	100
CT23	375	(191)	77.0	(104.5)	64.5	(1.64)	100

Table 5-2

Charpy V-Notch Impact Data for the V. C. Summer Unit 1 Reactor Vessel Weld Metal and HAZ Metal Irradiated at 550°F, Fluence 1.47×10^{19} n/cm^2 (E > 1.0 MeV)

Sample No.	Temperature (°F)	Temperature (°C)	Impact Energy (ft-lb)	Impact Energy (J)	Lateral Expansion (mils)	Lateral Expansion (mm)	Shear (%)
			Weld Metal				
CW17	-90	(-68)	22.0	(30.0)	22.5	(0.56)	10
CW25	-60	(-51)	19.0	(26.0)	17.5	(0.44)	15
CW23	-25	(-32)	10.0	(13.5)	16.0	(0.41)	15
CW20	-25	(-32)	10.0	(13.5)	14.5	(0.37)	20
CW19	-10	(-23)	37.0	(50.0)	32.0	(0.81)	30
CW26	0	(-18)	33.0	(44.5)	31.5	(0.80)	45
CW24	0	(-18)	42.0	(57.0)	36.5	(0.93)	45
CW30	25	(- 4)	29.0	(39.5)	28.5	(0.72)	35
CW18	25	(- 4)	46.0	(62.5)	42.0	(1.07)	70
CW27	50	(10)	62.0	(84.0)	54.5	(1.38)	70
CW28	50	(10)	78.0	(106.0)	65.0	(1.65)	95
CW29	100	(38)	73.0	(99.0)	63.0	(1.60)	95
CW21	150	(66)	84.0	(114.0)	72.5	(1.84)	100
CW22	200	(93)	79.0	(107.0)	68.5	(1.74)	100
CW16	300	(149)	92.0	(124.5)	85.5	(2.17)	100
			HAZ Metal				
CH28	-90	(-68)	22.0	(30.0)	19.0	(0.48)	10
CH26	-60	(-51)	26.0	(35.5)	20.0	(0.51)	15
CH27	-50	(-46)	27.0	(36.5)	24.0	(0.61)	20
CH29	-25	(-32)	26.0	(35.5)	26.0	(0.66)	20
CH25	-25	(-32)	24.0	(32.5)	21.5	(0.55)	20
CH30	-10	(-23)	77.0	(104.5)	52.0	(1.32)	50
CH23	-10	(-23)	41.0	(55.5)	31.0	(0.79)	30
CH18	0	(-18)	68.0	(92.0)	49.5	(1.26)	60
CH22	0	(-18)	63.0	(85.5)	47.5	(1.21)	50
CH17	50	(10)	112.0	(152.0)	77.0	(1.96)	100
CH19	50	(10)	72.0	(97.5)	52.5	(1.33)	65
CH21	100	(38)	95.0	(129.0)	73.5	(1.87)	95
CH24	150	(66)	112.0	(152.0)	76.0	(1.93)	100
CH16	200	(93)	103.0	(139.5)	74.0	(1.88)	100
CH20	300	(149)	117.0	(159.0)	84.0	(2.13)	100

Table 5-3

Instrumented Charpy Impact Test Results for V. C. Summer Unit 1
Shell Plate A9154-1 Irradiated at 1.47×10^{19} n/cm^2 (E > 1.0 MeV)

Sample Number	Test Temp (°F)	Charpy Energy (ft-lb)	Normalized Energies (ft-lb/in^2) Charpy Ed/A	Maximum Em/A	Prop Ep/A	Yield Load (kips)	Time to Yield (μsec)	Maximum Load (kips)	Time to Maximum (μsec)	Fracture Load (kips)	Arrest Load (kips)	Yield Stress (ksi)	Flow Stress (ksi)
						Longitudinal Orientation							
CL19	0	6.0	48	30	18	3.2	85	3.80	110	3.80	-	106	116
CL30	25	24.0	193	172	21	3.25	85	4.25	395	4.25	-	108	124
CL28	25	32.0	258	232	26	3.50	95	4.60	500	4.60	-	116	134
CL20	50	38.0	306	231	75	3.40	95	4.55	505	4.55	.15	113	132
CL22	50	44.0	354	318	36	3.45	85	4.65	650	4.65	-	114	134
CL29	77	73.0	588	303	285	3.15	90	4.35	665	4.10	1.20	105	124
CL26	78	79.0	636	308	328	3.25	85	4.50	655	3.95	.55	107	128
CL21	100	23.0	185	88	97	3.15	85	3.65	235	3.65	1.10	104	112
CL16	100	70.0	564	306	258	3.10	80	4.45	650	4.15	1.00	103	126
CL18	125	65.0	523	294	229	3.00	85	4.30	655	4.05	2.00	99	120
CL24	150	100.0	805	304	501	3.10	90	4.40	670	2.75	1.65	102	124
CL23	200	125.0	1007	269	737	2.70	75	4.00	635	-	-	89	111
CL17	250	121.0	974	295	679	2.9	35	4.20	670	-	-	95	117
CL25	350	119.0	958	289	670	2.75	90	4.00	675	-	-	91	112
CL27	400	125.0	1007	297	709	2.85	95	4.10	685	-	-	94	115
						Transverse Orientation							
CT21	-50	5.0	40	29	12	3.45	80	4.00	95	3.95	-	115	124
CT19	0	14.0	113	107	5	3.65	85	4.10	250	4.10	-	121	128
CT24	50	25.0	201	161	40	3.30	85	4.15	370	4.10	-	110	123
CT18	50	44.0	354	115	239	3.45	90	4.00	280	4.00	.40	113	123
CT16	77	35.0	282	155	127	3.15	85	3.95	375	3.95	1.35	105	118
CT30	78	33.0	266	176	90	3.20	90	4.30	405	4.20	.95	106	124
CT20	100	40.0	322	217	105	3.05	80	4.15	495	4.15	1.40	101	120
CT28	100	44.0	355	-	-	-	-	-	-	-	-	-	-
CT22	125	34.0	274	137	137	3.15	110	3.90	360	3.75	1.25	103	117
CT27	125	46.0	370	218	152	3.05	85	4.15	505	4.00	1.20	100	119
CT17	150	52.0	419	214	205	3.05	85	4.10	500	4.05	2.15	100	118
CT25	200	67.0	540	-	-	-	-	-	-	-	-	-	-
CT26	250	77.0	620	223	397	3.10	90	4.30	500	-	-	103	122
CT29	300	73.0	588	197	391	2.70	80	3.90	475	-	-	89	110
CT23	375	77.0	620	200	420	2.75	100	3.80	505	-	-	91	108

Table 5-4

Instrumented Charpy Impact Test Results for V_{19}C. Summer Unit 1
Weld Metal and HAZ Metal Irradiated AT 1.47×10^{19} n/cm (E > 1.0 MeV)

Sample Number	Test Temp (°F)	Charpy Energy (ft-lb)	Normalized Energies Charpy Ed/A (ft-lb/in²)	Maximum Em/A (ft-lb/in²)	Prop Ep/A (ft-lb/in²)	Yield Load (kips)	Time to Yield (μsec)	Maximum Load (kips)	Time to Maximum (μsec)	Fracture Load (kips)	Arrest Load (kips)	Yield Stress (ksi)	Flow Stress (ksi)
							Weld Metal						
CW17	- 90	22.0	177	71	106	3.90	90	4.35	175	4.30	-	128	136
CW25	- 60	19.0	153	124	29	3.80	90	4.50	275	4.45	-	126	137
CW23	- 25	10.0	81	44	36	3.50	85	3.80	130	3.80	.65	115	121
CW20	- 25	10.0	81	44	37	3.60	90	3.80	130	3.75	.30	119	123
CW19	- 10	37.0	298	249	49	3.70	90	4.60	510	4.50	.35	123	137
CW26	0	33.0	266	198	68	3.60	90	4.35	430	4.35	1.05	118	131
CW24	0	42.0	338	244	95	3.65	90	4.60	505	4.55	.75	121	137
CW30	25	29.0	234	112	121	3.45	90	4.00	275	3.95	2.35	114	124
CW18	25	46.0	370	234	136	3.35	85	4.30	510	4.20	2.4	110	126
CW27	50	62.0	499	227	272	3.30	85	4.35	500	4.05	2.20	109	126
CW28	50	78.0	628	280	348	3.50	85	4.60	575	-	-	116	134
CW29	100	73.0	588	262	326	3.35	95	4.35	575	-	-	110	127
CW21	150	84.0	676	278	398	3.2	85	4.40	605	-	-	105	125
CW22	200	79.0	636	265	371	3.05	85	4.15	600	-	-	101	119
CW16	300	92.0	741	256	485	2.80	85	4.00	605	-	-	92	112
							HAZ Metal						
CH28	- 90	22.0	177	159	18	4.30	95	4.75	320	4.75	-	143	150
CH26	- 60	26.0	209	181	28	4.25	105	4.80	370	4.75	-	141	150
CH27	- 50	27.0	217	179	38	3.85	90	4.65	375	4.60	.25	127	140
CH25	- 25	24.0	193	152	41	3.80	90	4.40	330	4.40	.30	126	136
CH29	- 25	26.0	209	160	49	3.85	95	4.45	350	4.40	.55	128	138
CH23	- 10	41.0	330	294	36	3.90	110	4.80	595	4.65	1.45	129	144
CH30	- 10	77.0	620	339	281	3.85	85	4.85	655	4.45	2.00	127	144
CH22	0	63.0	507	291	216	3.90	95	4.80	580	4.65	1.45	129	144
CH18	0	68.0	548	333	214	3.75	90	4.85	655	4.75	2.80	125	143
CH19	50	72.0	580	325	255	3.55	135	4.75	700	4.65	2.60	117	137
CH17	50	112.0	902	317	585	3.45	90	4.60	665	-	-	114	133
CH21	100	95.0	765	263	502	3.30	90	4.35	575	-	-	109	127
CH24	150	112.0	902	312	590	3.40	90	4.55	660	-	-	112	132
CH16	200	103.0	829	297	533	3.15	85	4.30	660	-	-	104	123
CH20	300	117.0	944	-	-	-	-	-	-	-	-	-	-

Table 5-5

Effect of 550°F Irradiation at 1.47 x 10^{19} n/cm^2 (E > 1.0 MeV)
on Notch Toughness Properties of V. C. Summer Unit 1 Reactor Vessel Materials

Material	Average 30 ft-lb Temperature (°F) Unirradiated	Irradiated	ΔT	Average 35 mil Lateral Expansion Temperature (°F) Unirradiated	Irradiated	ΔT	Average 50 ft-lb Temperature (°F) Unirradiated	Irradiated	ΔT	Average Energy Absorption at Full Shear (ft-lb) Unirradiated	Irradiated	Δ(ft-lb)
Plate A9514-1 (Longitudinal)	-25	35	60	0	50	50	0	65	65	132	122	10
Plate A9514-1 (Transverse)	25	65	40	55	95	40	75	130	55	75	76	1[(a)]
Weld Metal	-60	-15	45	-35	0	35	-15	30	45	91	85	6
HAZ Metal	-90	-45	45	-60	-15	45	-70	-15	55	130	111	19

(a) Increase in shelf energy

Table 5-6

Comparison of V. C. Summer Unit 1, 30 ft-lb Transition Temperature
Results with Regulatory Guide 1.99 Revision 2 Prediction

Material	Capsule	Fluence	R.G. 1.99 Rev. 2 Predicted 30 ft-lb Transition Temperature Shift	Actual Shift Based On Surveillance Data
Plate A9514-1 (Longitudinal)	U	6.39×10^{18}	57°F	40°F
	V	1.47×10^{19}	72°F	60°F
Plate A9514-1 (Transverse)	U	6.39×10^{18}	57°F	30°F
	V	1.47×10^{19}	72°F	40°F
Weld Metal	U	6.39×10^{18}	59°F	30°F
	V	1.47×10^{19}	75°F	45°F

Table 5-7

Tensile Properties for V. C. Summer Unit 1 Reactor Vessel Material
Irradiated at 550°F to 1.47×10^{19} n/cm^2 (E > 1.0 MeV)

Sample Number	Material	Test Temp. (°F)	0.2% Yield Strength (ksi)	Ultimate Strength (ksi)	Fracture Load (kip)	Fracture Stress (ksi)	Fracture Strength (ksi)	Uniform Elongation (%)	Total Elongation (%)	Reduction in Area (%)
CL5	Long.	100	69.0	91.7	3.05	212.1	62.1	12.0	25.4	71
CL4	Long.	250	68.2	86.6	2.90	201.7	59.1	11.3	23.9	71
CL6	Long.	550	61.6	88.6	3.05	194.8	62.1	10.5	23.0	63
CT6	Trans.	74	69.3	92.7	3.33	168.1	67.8	12.8	26.0	60
CT4	Trans.	200	65.5	87.6	3.10	162.4	63.2	10.5	21.9	61
CT5	Trans.	550	61.1	88.2	3.45	211.5	70.3	10.5	19.2	67
CW6	Weld	0	81.0	98.8	3.30	202.3	67.2	13.5	25.8	67
CW5	Weld	100	76.9	91.7	3.00	176.5	61.1	12.0	23.4	65
CW4	Weld	550	70.3	88.6	3.25	152.5	66.2	9.8	19.4	57

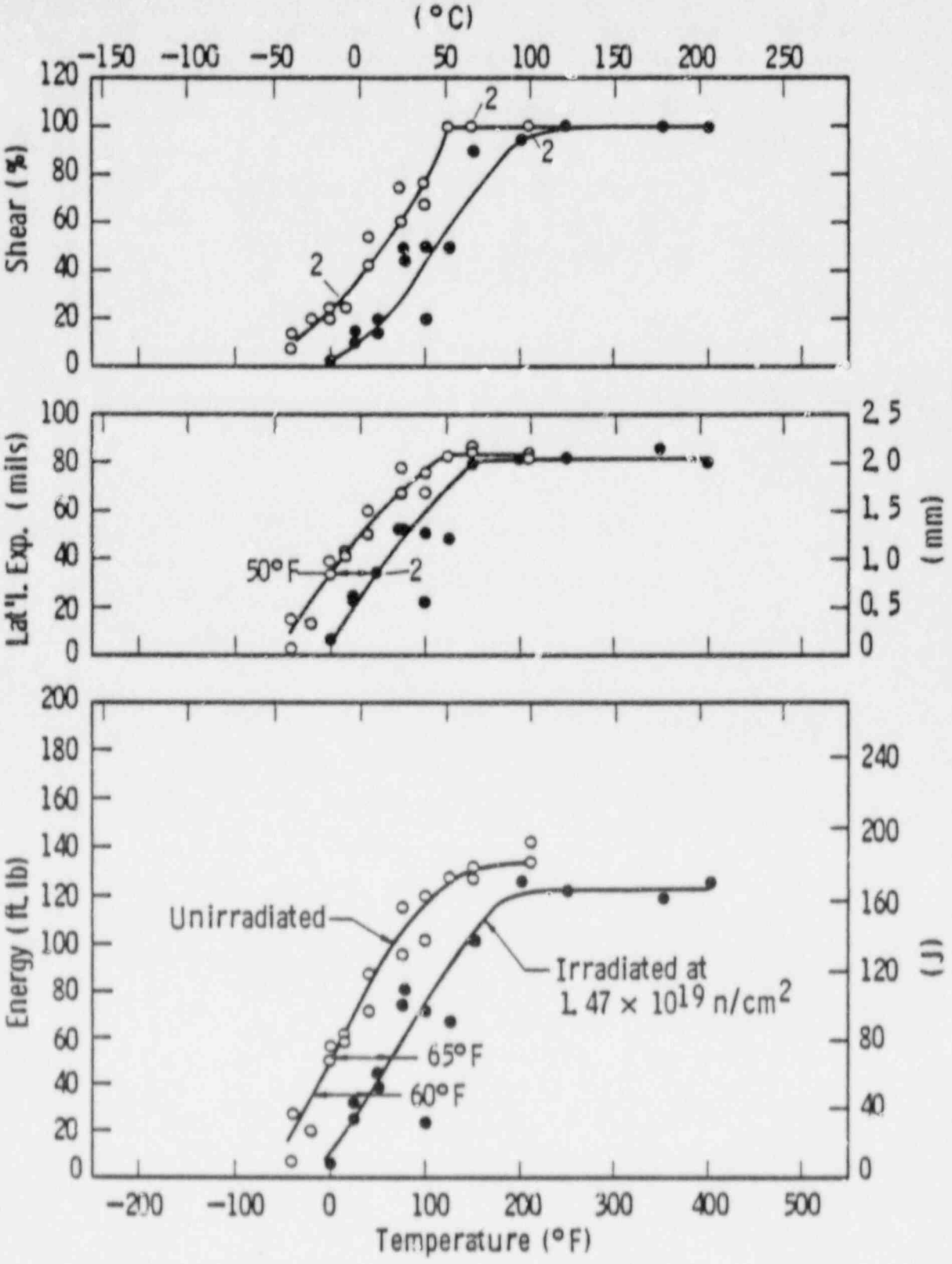

Figure 5-1. Charpy V-notch impact properties for V. C. Summer Unit 1 reactor vessel shell plate A9154-1 (longitudinal orientation)

Curve 755039-A

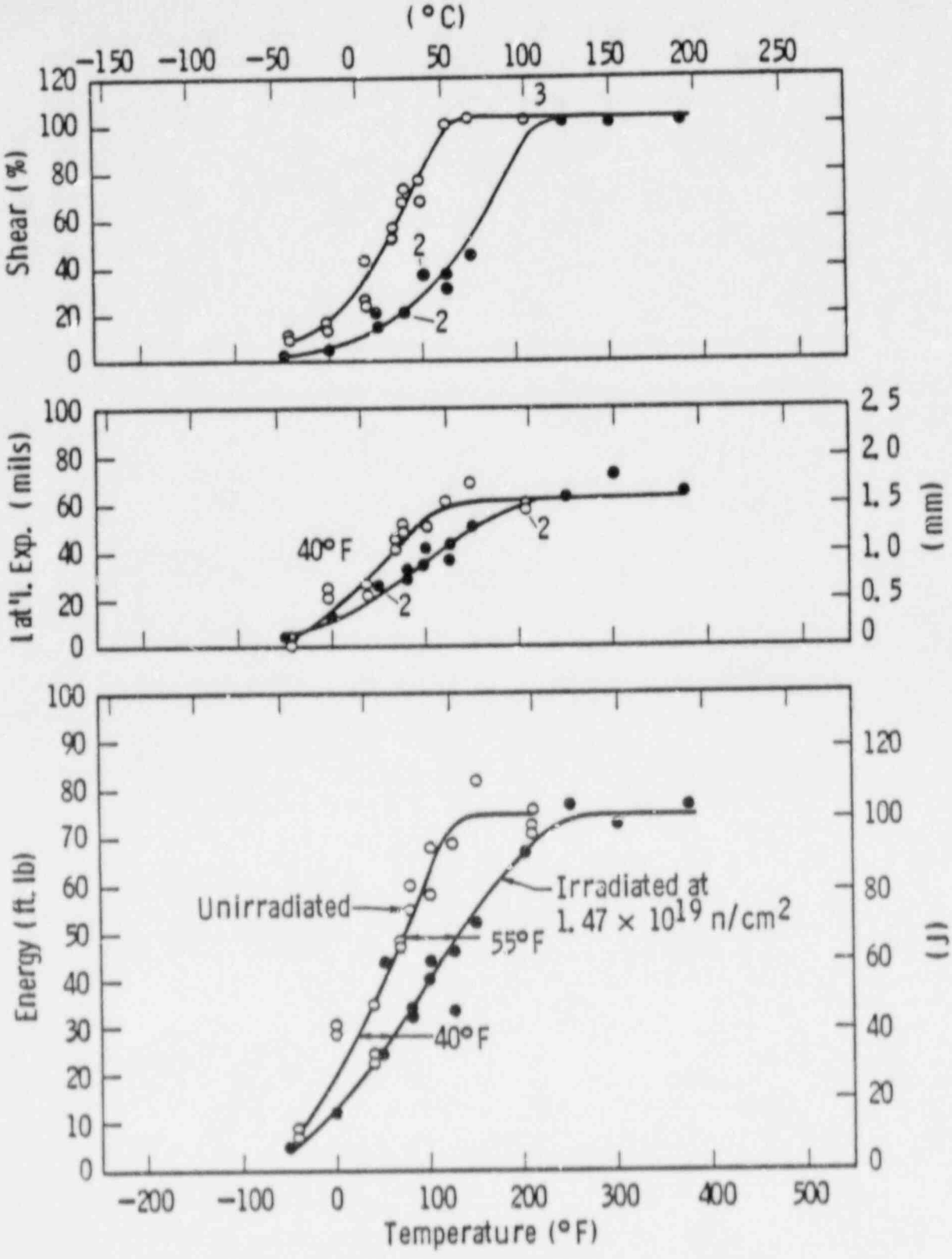

Figure 5-2. Charpy V-notch impact properties for V. C. Summer Unit 1 reactor vessel shell plate A9154-1 (transverse orientation)

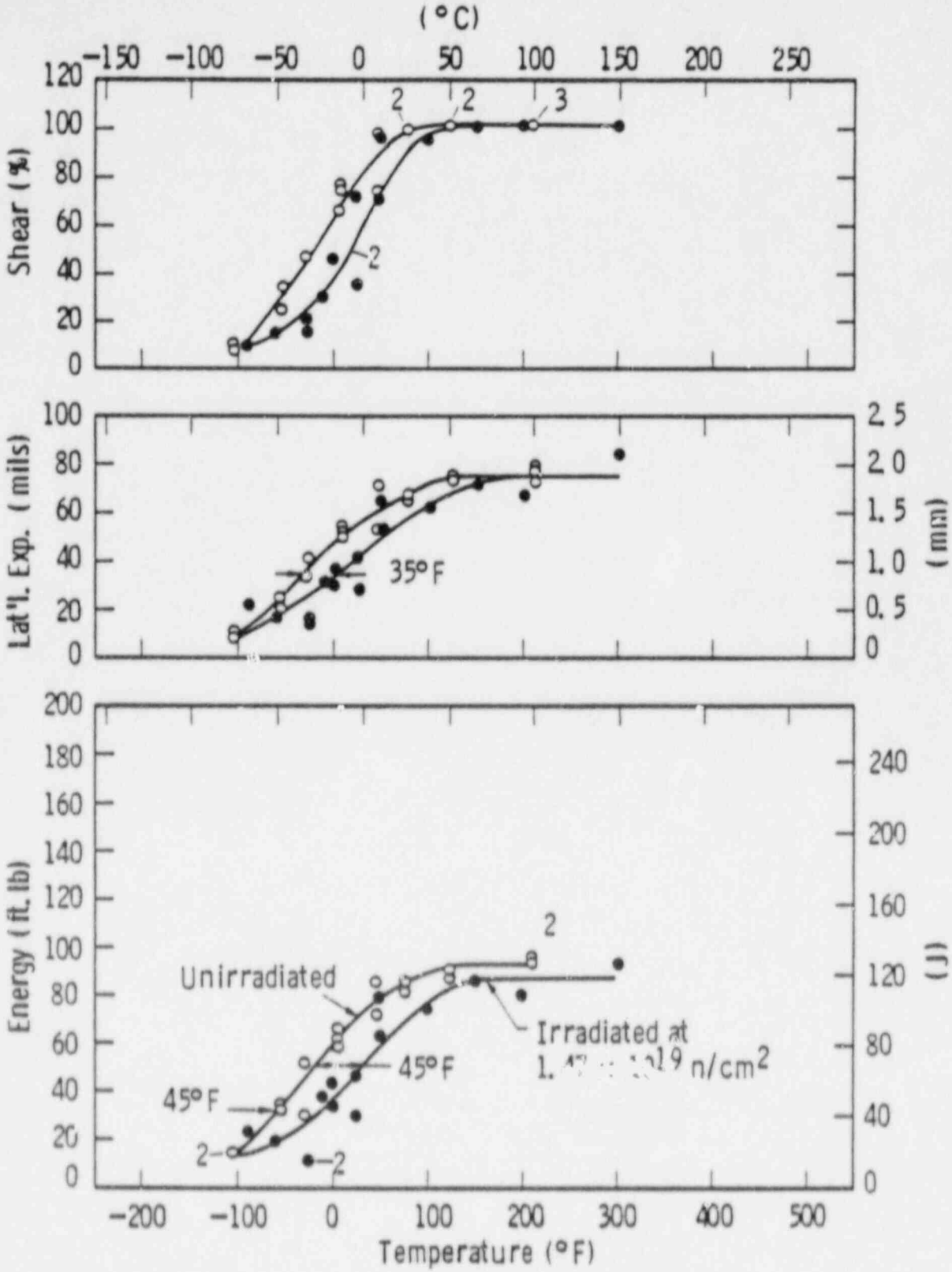

Figure 5-3. Charpy V-notch impact properties for V. C. Summer Unit 1 reactor vessel weld metal

Curve 755038-A

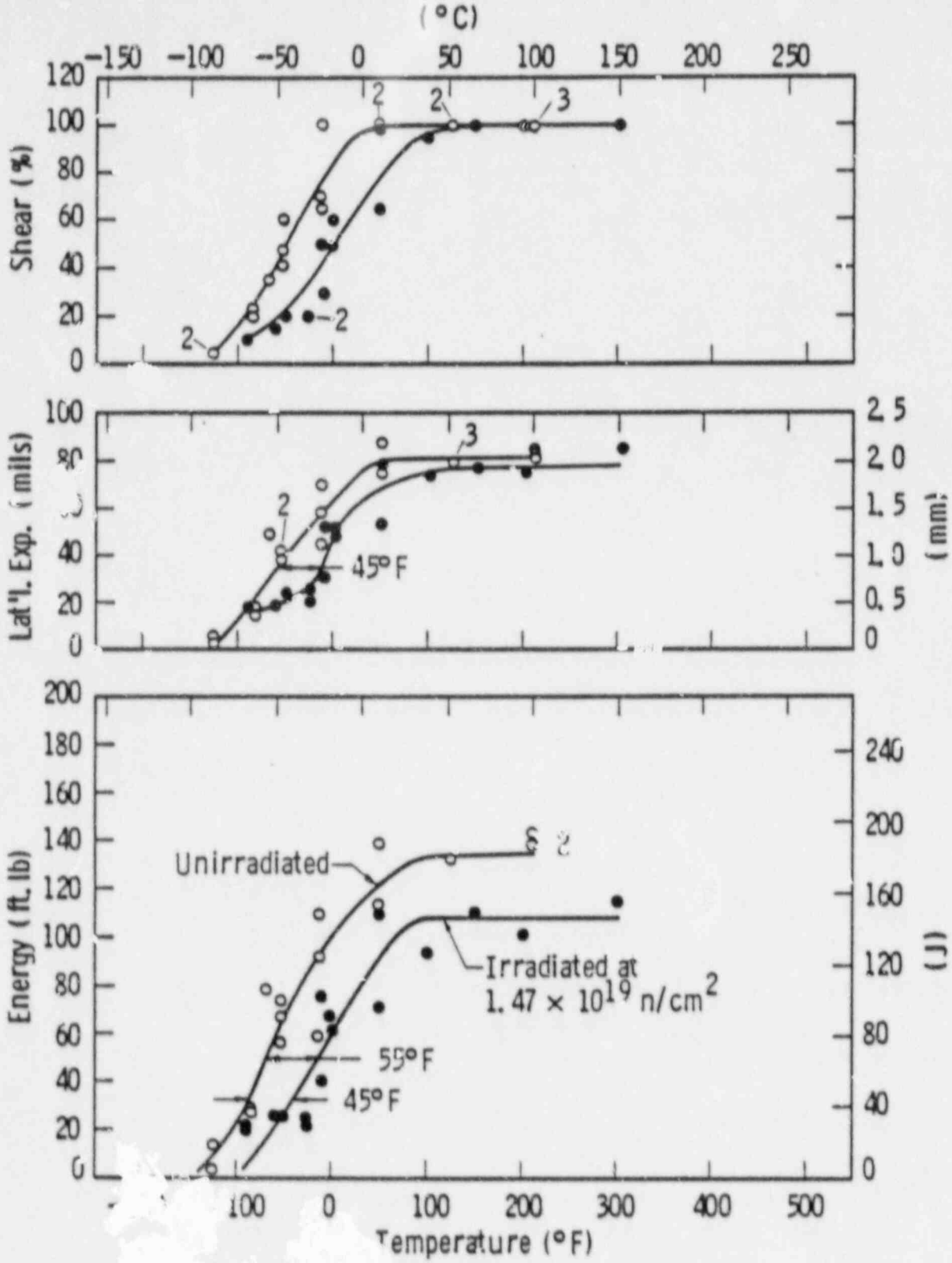

Figure [illegible] Impact properties for V. C. Summer Unit 1 weld heat affected zone metal

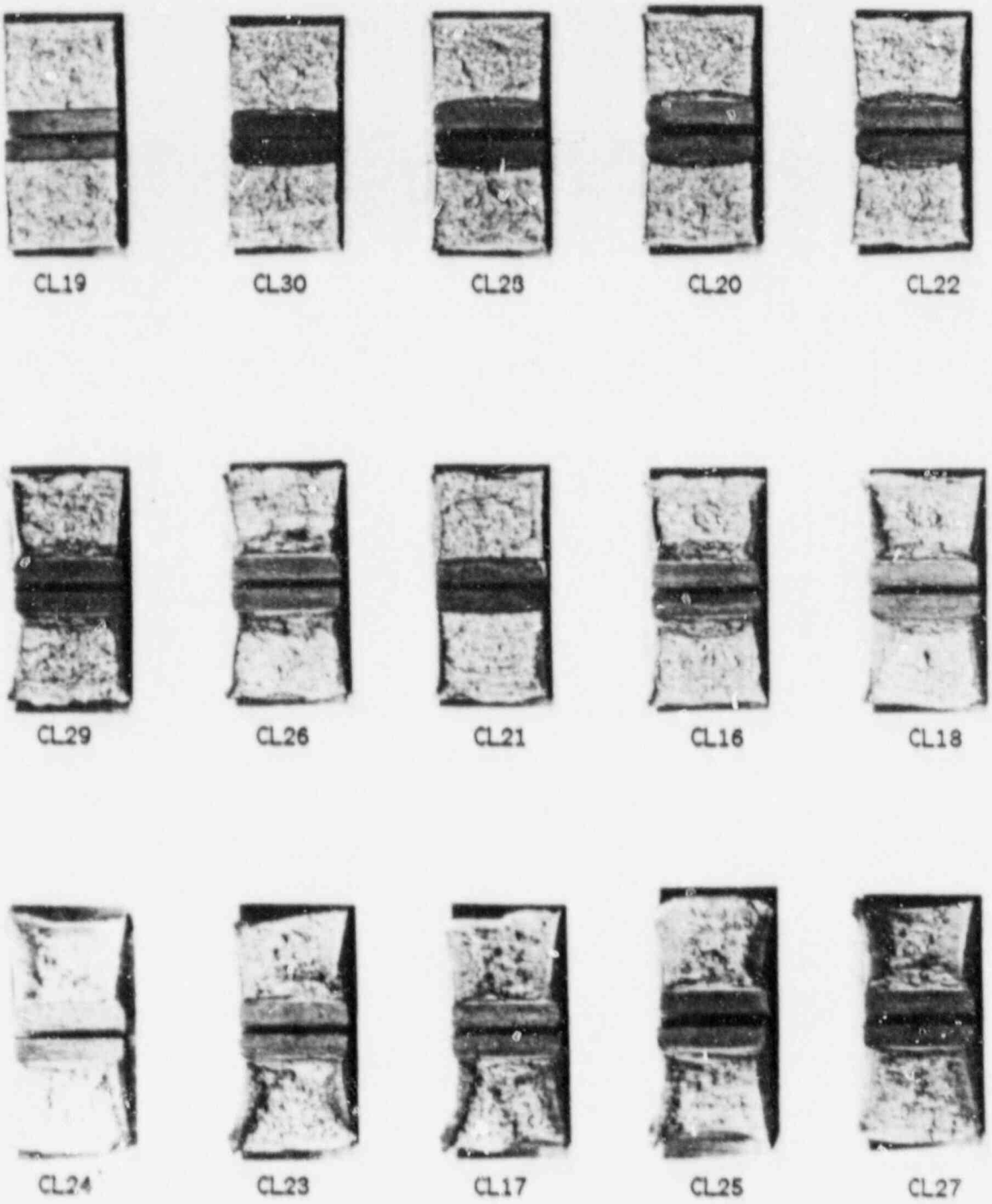

Figure 5-5. Charpy impact specimen fracture surfaces for V. C. Summer Unit 1 reactor vessel shell Plate A9154-1 (longitudinal orientation)

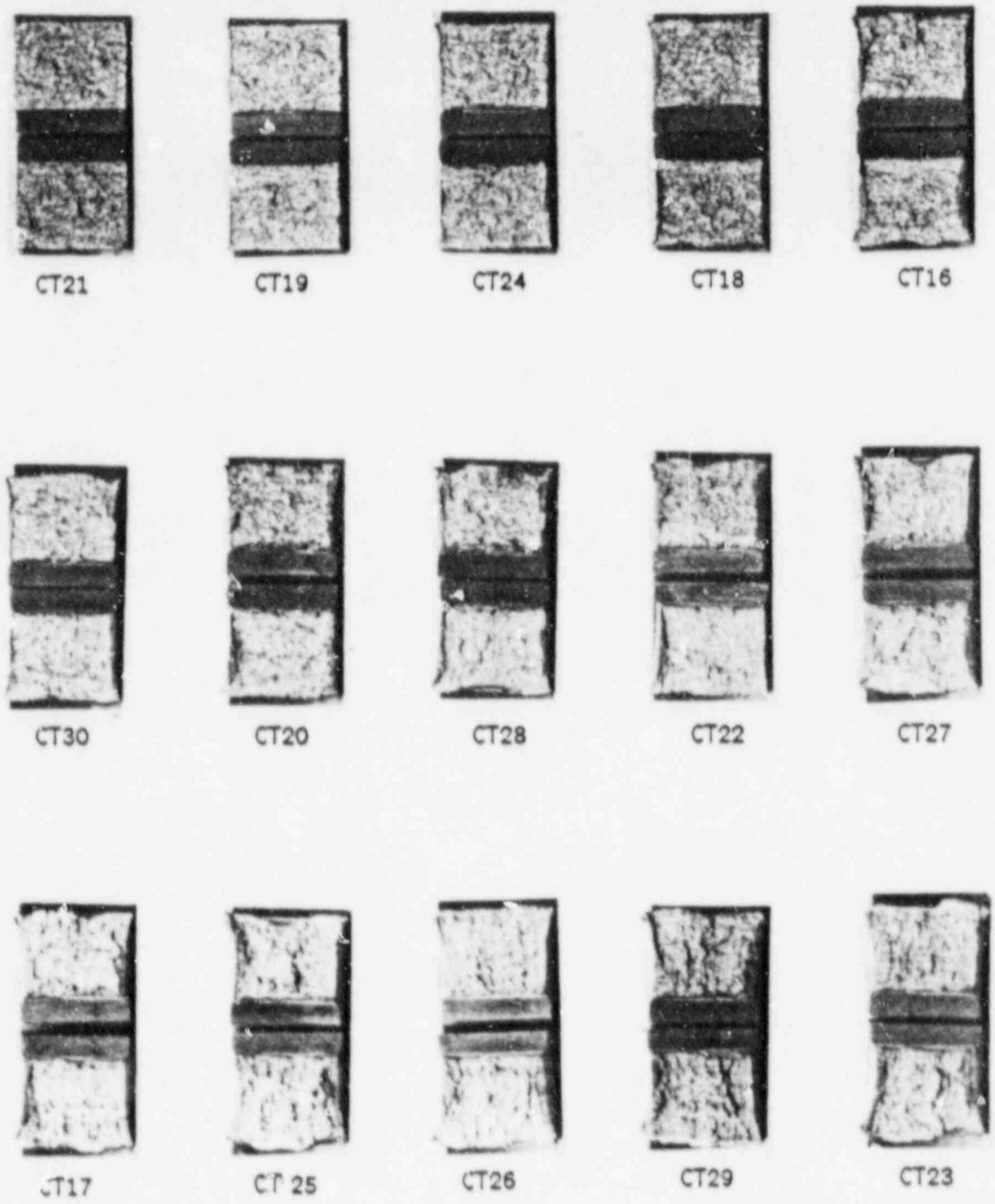

Figure 5-6. Charpy impact specimen fracture surfaces for V. C. Summer Unit 1 reactor vessel shell plate A9154-1 (transverse orientation)

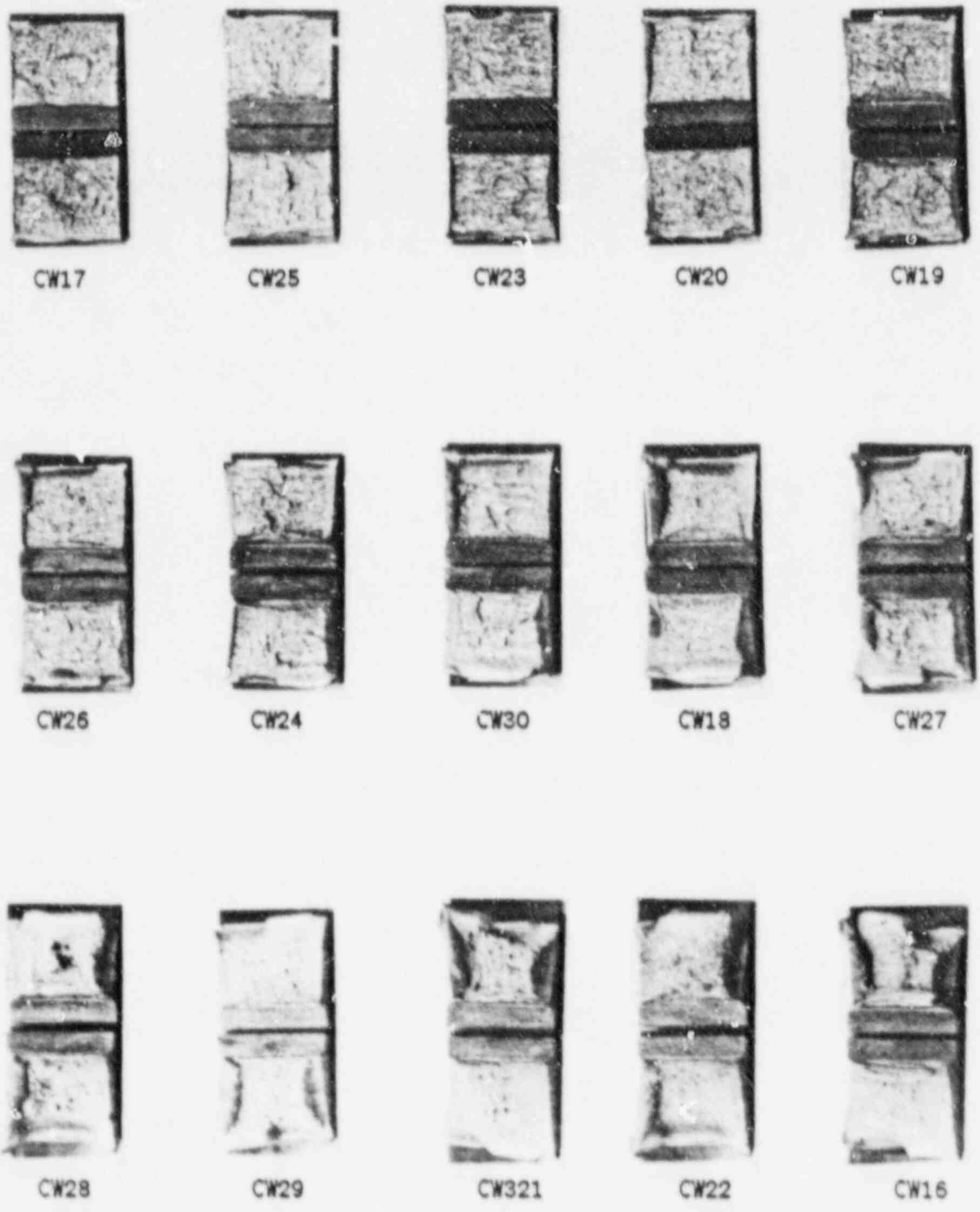

Figure 5-7. Charpy impact specimen fracture surfaces for V. C. Summer Unit 1 reactor vessel weld metal

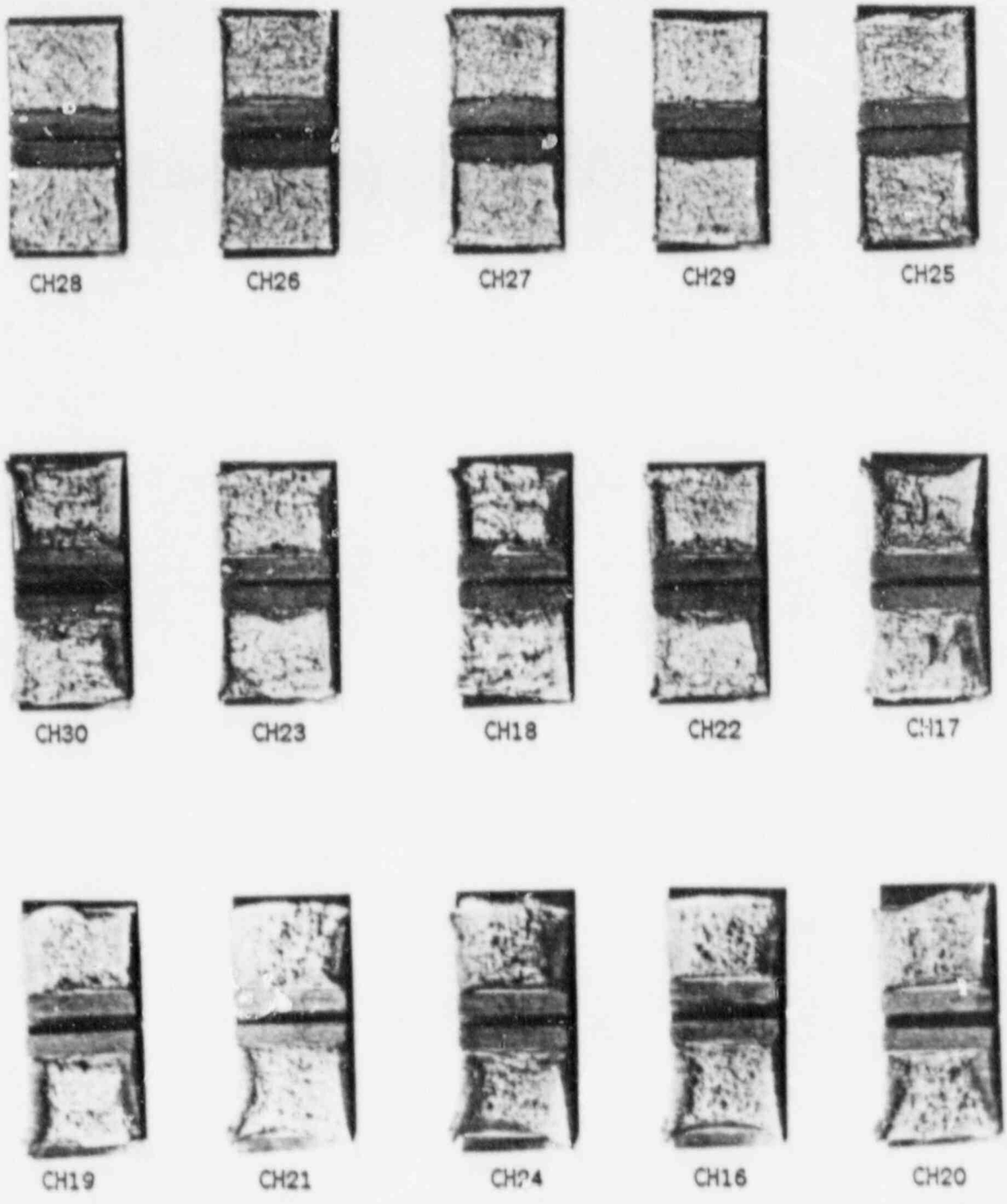

Figure 5-8. Charpy impact specimen fracture surfaces for V. C. Summer Unit 1 reactor vessel weld heat affected zone metal

Curve 755035-A

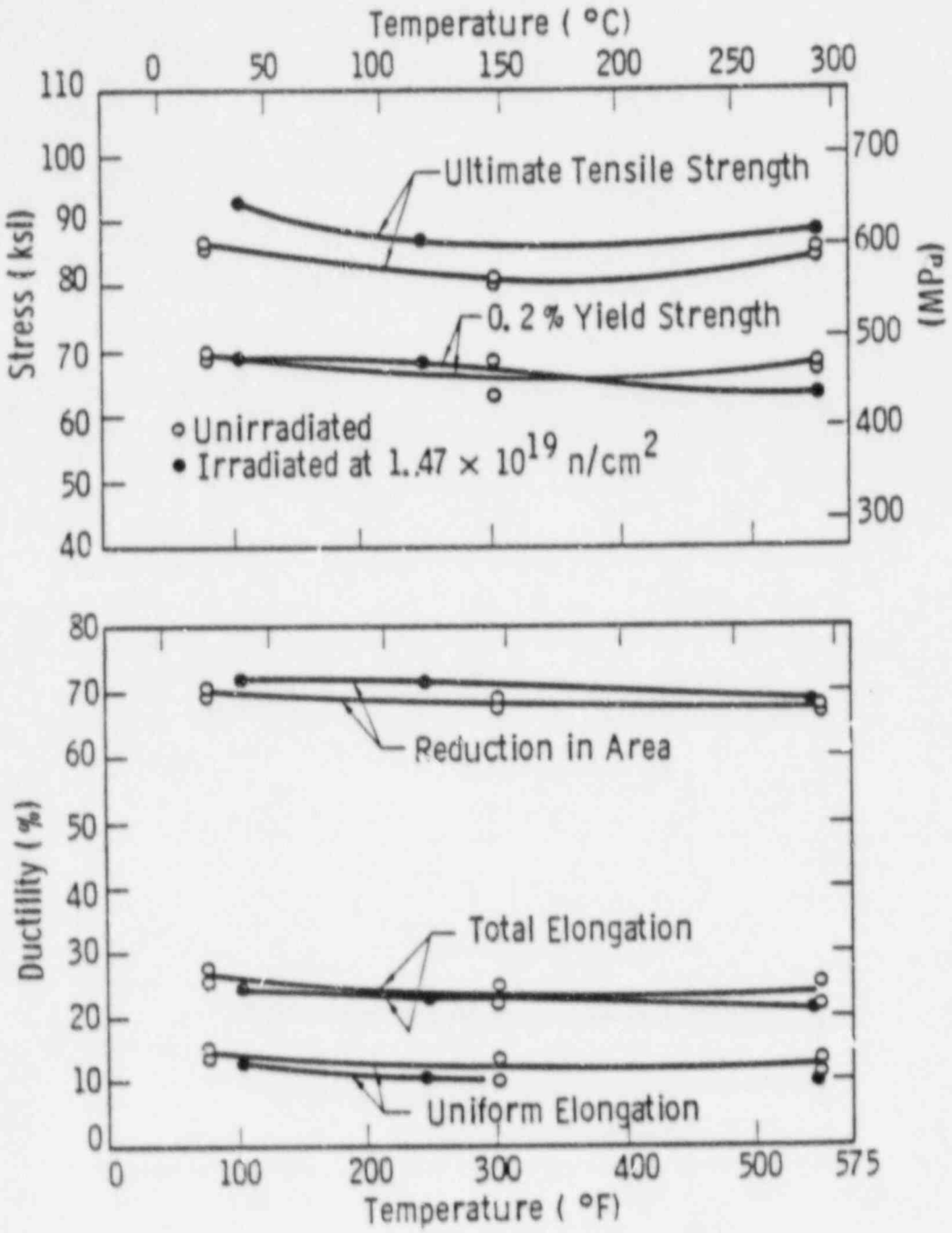

Figure 5-9. Tensile properties for V. C. Summer Unit 1 reactor vessel shell plate A9154-1 (longitudinal orientation)

Curve 755036-A

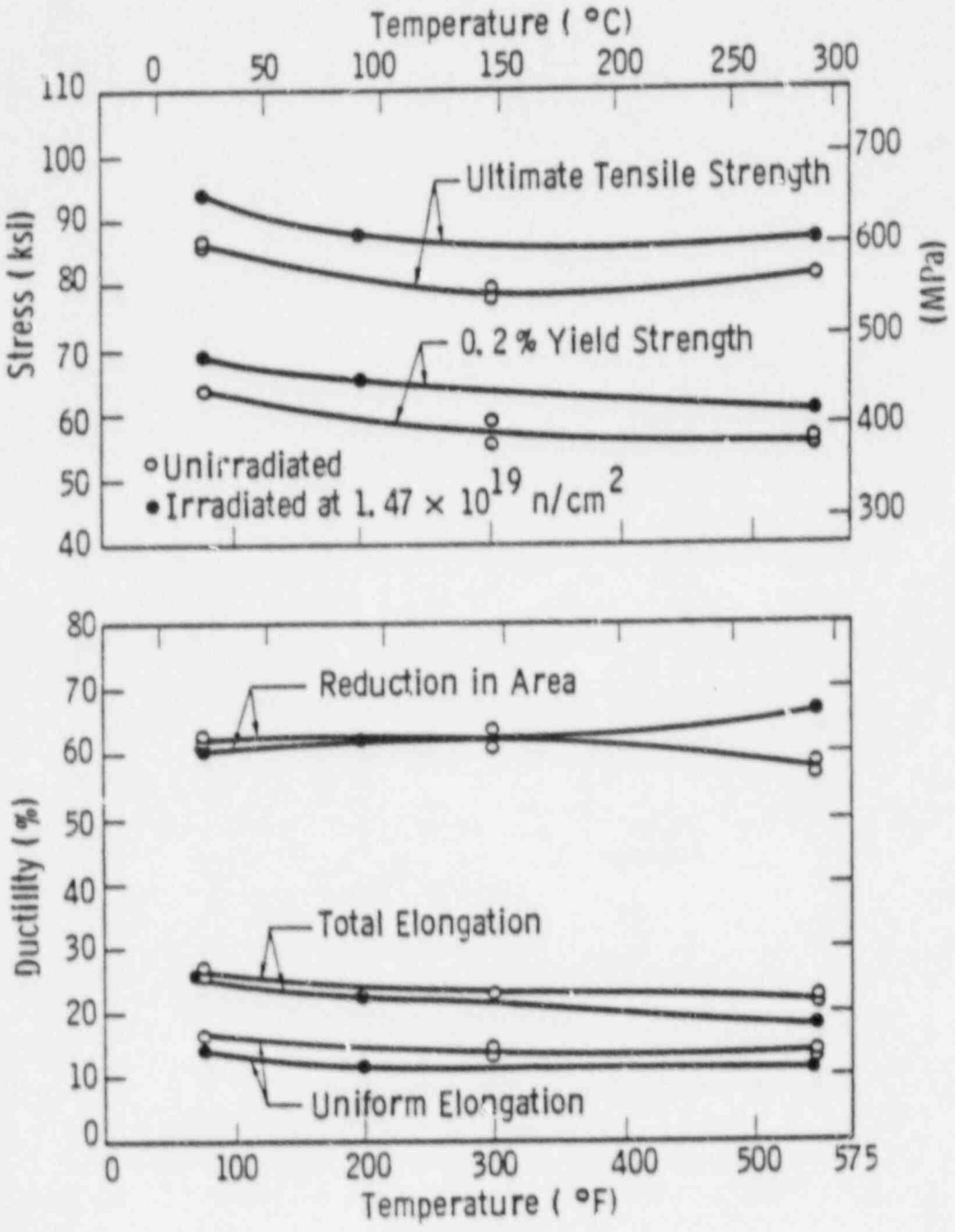

Figure 5-10. Tensile properties for V. C. Summer Unit 1 reactor vessel shell plate A9154-1 (transverse orientation)

Curve 755034-A

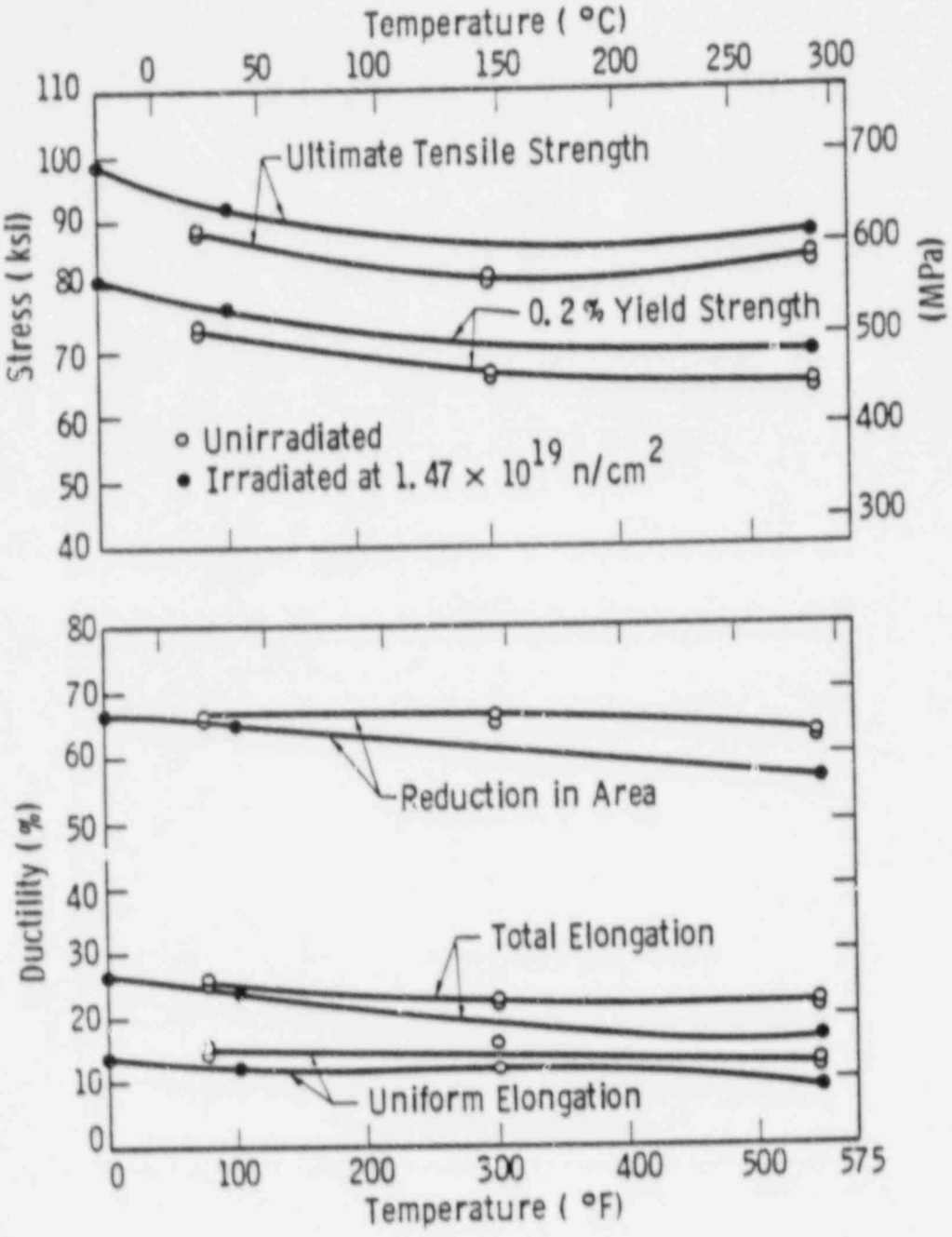

Figure 5-11. Tensile properties for V. C. Summer Unit 1 reactor vessel weld metal

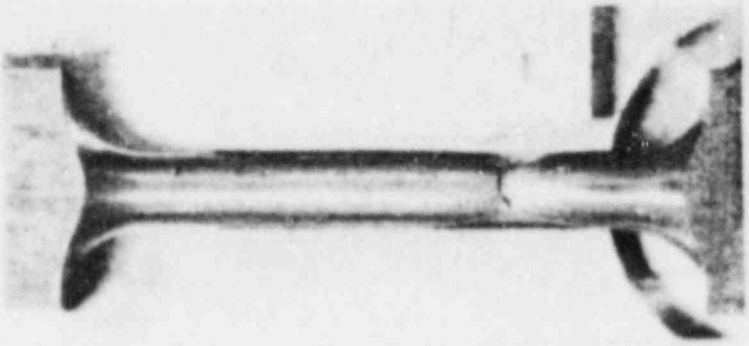

Specimen CL5 100°F

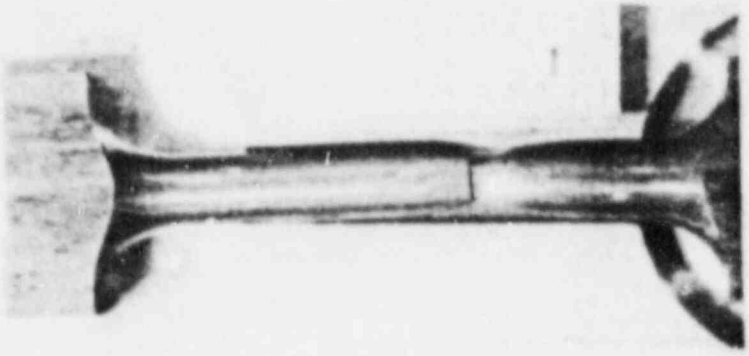

Specimen CL4 250°F

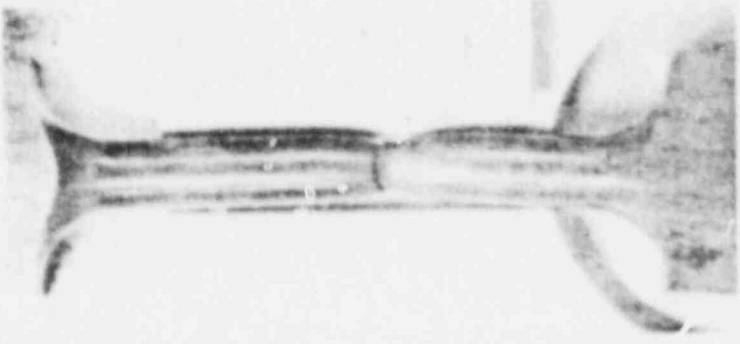

Specimen CL6 550°F

Figure 5-12. Fractured tensile specimens from V. C. Summer Unit 1 reactor vessel shell plate A9154-1 (longitudinal orientation)

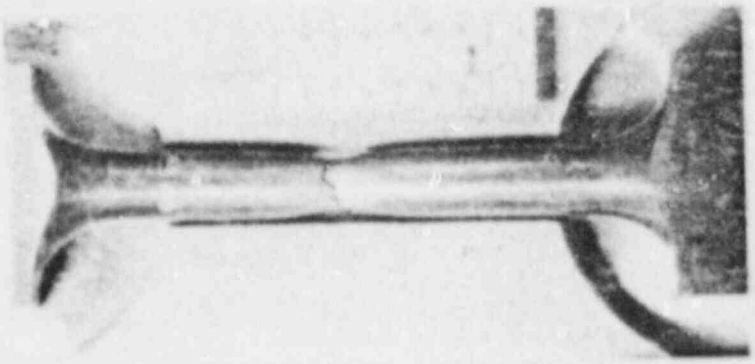

Specimen CT6 74°F

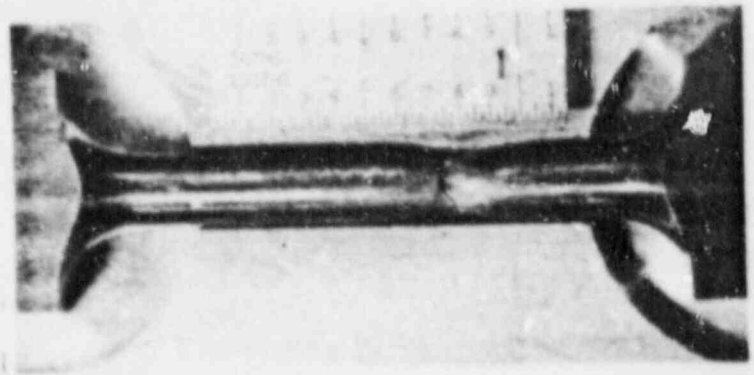

Specimen CT4 200°F

Specimen CT5 550°F

Figure 5-13. Fractured tensile specimens from V. C. Summer Unit 1 reactor vessel shell plate A9154-1 (transverse orientation)

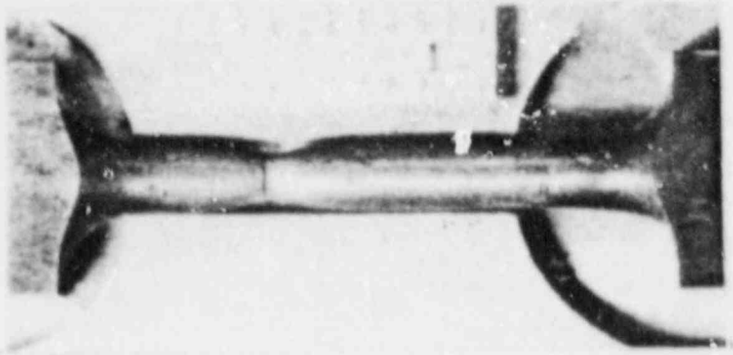

Specimen CW6 0°F

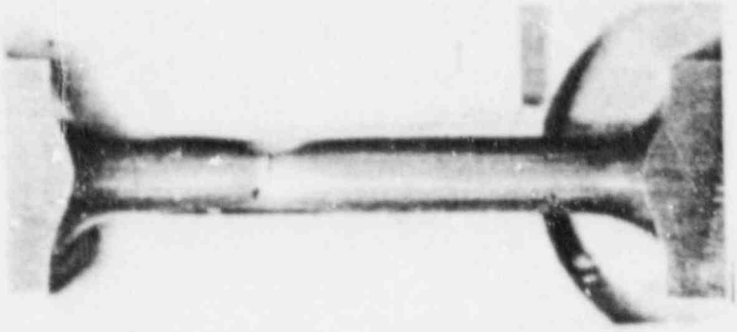

Specimen CW5 100°F

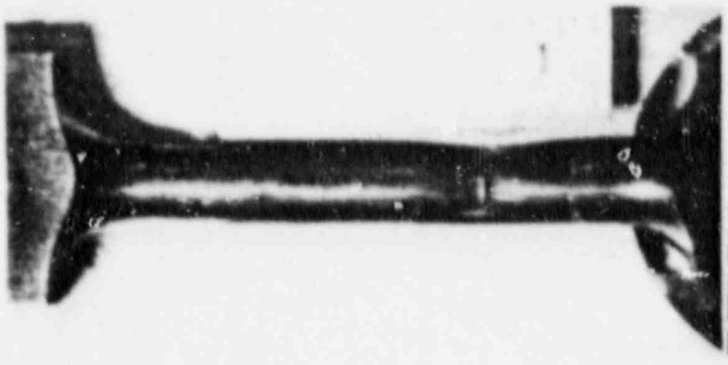

Specimen CW4 550°F

Figure 5-14. Fractured tensile specimens from V. C. Summer Unit 1 reactor vessel weld metal

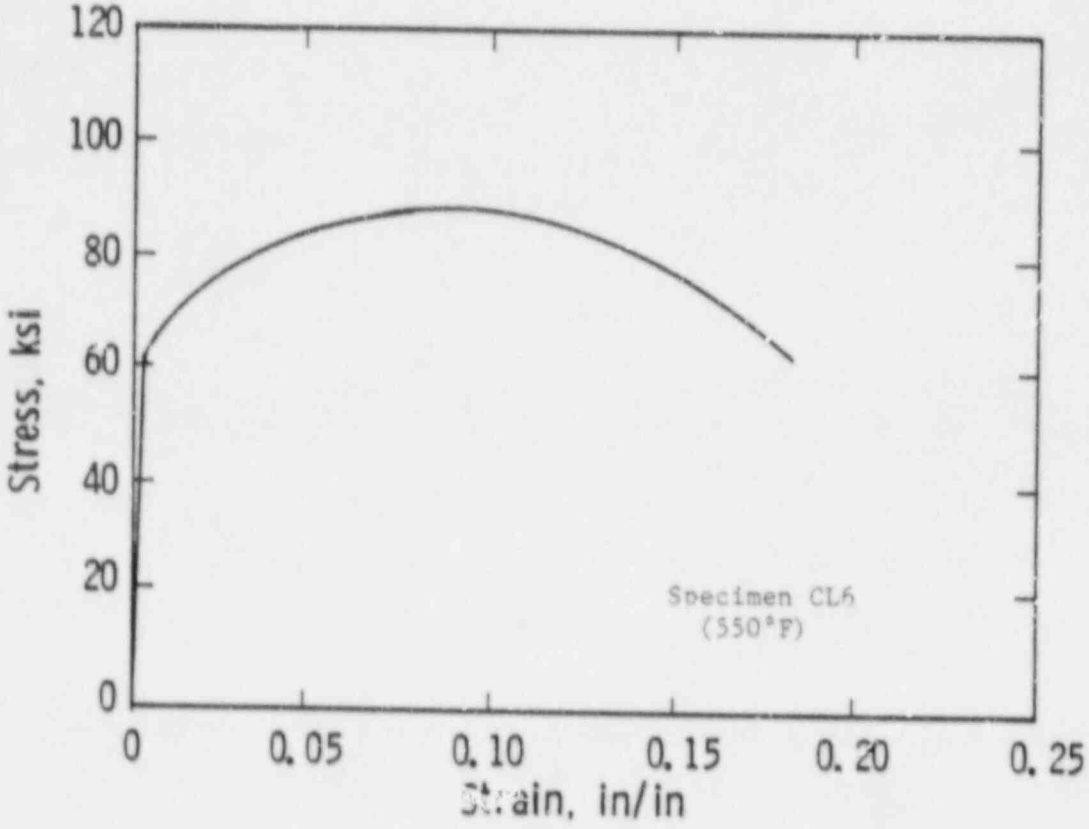

Figure 5-15. Typical stress-strain curve for tension specimens

6. RADIATION ANALYSIS AND NEUTRON DOSIMETRY

6.1 INTRODUCTION

Knowledge of the neutron environment within the reactor pressure vessel and surveillance capsule geometry is required as an integral part of LWR reactor pressure vessel surveillance programs for two reasons. First, in order to interpret the neutron radiation-induced material property changes observed in the test specimens, the neutron environment (energy spectrum, flux, fluence) to which the test specimens were exposed must be known. Second, in order to relate the changes observed in the test specimens to the present and future condition of the reactor vessel, a relationship must be established between the neutron environment at various positions within the reactor vessel and that experienced by the test specimens. The former requirement is normally met by employing a combination of rigorous analytical techniques and measurements obtained with passive neutron flux monitors contained in each of the surveillance capsules. The latter information is derived solely from analysis.

This section describes a discrete ordinates S_n transport analysis performed for the V. C. Summer Unit 1 reactor to determine the fast (E > 1.0 MeV) neutron flux and fluence as well as the neutron energy spectra within the reactor vessel and surveillance capsules. The analysis data were then used to develop lead factors for use in relating neutron exposure of the reactor vessel to that of the surveillance capsules. Based on the use of spectrum-averaged reaction cross sections derived from this calculation and the V. C. Summer Unit 1 power history, the analysis of the neutron dosimetry contained in Capsule V and an updated evaluation of dosimetry from Capsule U is presented.

6.2 DISCRETE ORDINATES ANALYSIS

A plan view of the V. C. Summer Unit 1 geometry at the core midplane is shown in Figure 6-1. Since the reactor exhibits 1/8 the core symmetry, only zero to 45-degree sector is depicted. Six irradiation capsules attached to the neutron pads are included in the design to constitute the reactor vessel surveillance program. The capsules are located at 16.94 and 19.72 from the major axis at 0° shown in Figure 6-1.

A plan view of a single surveillance capsule attached to the neutron pads is shown in Figure 6-2. The stainless steel specimen container is 1.182 by 1-inch and approximately 56 inches in height. The containers are positioned axially such that the specimens are centered on the core midplane, thus spanning the central 5 feet of the 12-foot-high reactor core.

From a neutron transport standpoint, the surveillance capsule structures are significant. They have a marked effect on both the distribution of neutron flux and the neutron energy spectrum in the water annulus between the thermal shield and the reactor vessel. In order to properly determine the neutron environment at the test specimen locations, the capsules themselves must be included in the analytical model. This requires at least a two-dimensional calculation.

In the analysis of the neutron environment within the V. C. Summer Unit 1 reactor geometry, two sets of transport calculations were carried out. The first, a single calculation in the conventional forward mode, was used to obtain spectrum-averaged reaction cross sections and gradient corrections for dosimetry reactions. The second set of calculations consisted of a series of adjoint mode neutron transport calculations relating the fast ($E > 1.0$ MeV) neutron flux at the surveillance capsule locations and at selected azimuthal locations on the reactor vessel to the power distributions in the reactor core. These adjoint importance functions, when combined with cycle-specific core power distributions, yield plant-specific fast neutron exposure at the surveillance capsule and pressure vessel locations for each operating fuel cycle.

The forward transport calculation was carried out in R, θ geometry with an S_6 angular quadrature using the DOT two dimensional discrete ordinates code[4] and the SAILOR cross-section library.[5] The SAILOR library is a 47 group, ENDF-B/V based data set which was developed specifically for light water reactor applications. Anisotropic scattering is treated with a P_3 expansion of the scattering cross-sections. The energy group structure used in the analysis is listed in Table 6-1.

The design basis core power distribution used in the transport calculation was derived from statistical studies of long-term operation of Westinghouse 3-loop plants. Inherent in the development of this design basis core power distribution is the use of an out-in fuel management strategy; i.e., fresh fuel on the core periphery. Furthermore, for the peripheral fuel assemblies, a 2σ uncertainty derived from the statistical evaluation of plant to plant and cycle to cycle variations in peripheral power was used. Since it is unlikely that a single reactor would have a power distribution at the nominal $+2\sigma$ level for a large number of fuel cycles, the use of this design basis distribution is expected to yield conservative results. This is especially true in cases where low leakage fuel management has been employed.

The adjoint analyses were also carried out using the 47 neutron energy group, P_3 cross sections from the SAILOR library and an S_6 angular quadrature. Adjoint source locations were chosen at the center of each of the surveillance capsules as well as at positions along the inner diameter of the pressure vessel. These calculations were run in R, θ geometry to provide power distribution importance functions for the neutron exposure parameters of interest. Having the adjoint importance functions and appropriate core power distributions, the response of interest is calculated as

$$R_{R',\theta'} = \int_R \int_\theta \int_E I(R,\theta,E)\ F(R,\theta,E)\ dE d\theta R dR$$

where:

$R_{R',\theta'}$ = Response of interest (e.g., ϕ (E > 1.0 MeV), dpa, etc.) at radius R' and azimuthal angle θ'.

$I(R,\theta,E)$ = Adjoint importance function at radius R and azimuthal angle θ for neutron energy group E.

$F(R,\theta,E)$ = Full power fission neutron density at radius R and azimuthal angle θ for neutron energy group E.

The fission neutron density distributions used include the enrichment and burnup dependent effects of the fissions of other actinides in addition to U-235.

Core power distributions for use in the V. C. Summer plant specific evaluations are derived from measured assembly and cycle burnups for each operating fuel cycle to date. The adjoint results are in terms of fuel cycle averaged neutron flux which when multiplied by the fuel cycle length yields the incremental fast neutron fluence.

The core power distributions used in the plant specific fast neutron exposure analysis of the V. C. Summer surveillance capsule and reactor vessel were derived from the following fuel cycle nuclear design reports:

Fuel Cycle	Nuclear Design Report
1	WCAP-9685
2	WCAP-10663, Rev. 1
3	WCAP-10874

Three regions of the core consisting of subsets of fuel assemblies are defined. In performing the adjoint evaluations, the relative power in the fuel assemblies comprising region 3 has been adjusted to account for known biases in the prediction of power in the peripheral fuel assemblies while the relative power in the fuel assemblies comprising region 2 has been maintained at the cycle average value. Due to the extreme self-shielding of the reactor core, neutrons born in the fuel assemblies comprising region 1 do not contribute

significantly to the neutron exposure of either the surveillance capsules or the reactor vessel.

In each of the adjoint evaluations, within-assembly spatial gradients have been superimposed on the average assembly power levels. For the peripheral assemblies (Region 3), these spatial gradients also include adjustments to account for analytical deficiencies that tend to occur near the boundaries of the core region.

Reactor vessel and surveillance capsule neutron fluence projections are made to 32 effective full power years (EFPY). Current neutron fluences, based on past core loadings, are defined as of the end of Cycle 3.

Several key assumptions are required to make the neutron fluence projections. In particular the time weighted average neutron flux for Cycles 2 and 3 and an 80 percent capacity factor are assumed to be representative of all future operation. Thus, the neutron fluence projections reflect a continued commitment to the low leakage fuel management strategy shown by the second and third core loading. Finally, it is assume that the V. C. Summer core will continue to be operated at the current power level of 2775 MWt.

The Westinghouse neutron transport methodology, both forward and adjoint, using the SAILOR cross-section library has been benchmarked against the Oak Ridge National Laboratory (ORNL) Poolside Critical Assembly (PCA) facility,[6] the Venus PWR engineering Mockup,[7] and the Westinghouse power reactor surveillance capsule data base.[8] The benchmarking studies show that the use of SAILOR cross sections and design basis core power distributions produces neutron fluxes that tend to be conservative with calculation exceeding measurements by 10 to 25 percent. When plant specific core power distributions are used with the adjoint importance functions, the benchmarking studies show that neutron fluence predictions are distributed within plus or minus 15 percent of measured values at surveillance capsule locations. This analysis is consistent with established ASTM standards.[9-13]

6.3 RADIOMETRIC MONITORS

The passive radiometric monitors included in the V. C. Summer Unit 1 surveillance program are listed in Table 6-2. The first five reaction in Table 6-2 are used as fast neutron monitors to relate fast (E > 1.0 MeV) neutron fluence to measured material property changes. In order to assess the potential for burnout of the product nuclides generated by fast neutron reactions, it is necessary to also determine the magnitude of the thermal and resonance region neutron flux at the monitor location. Therefore, bare and cadmium-shielded cobalt-aluminum monitors are also included.

The relative locations of the various radiometric monitors within the surveillance capsule are shown in Figure 4-2. The iron, nickel, copper, and cobalt-aluminum monitors, in wire form, are placed in holes drilled in spacers at several axial levels within the capsules. The cadmium-shielded neptunium and uranium fission monitors are accommodated within the dosimeter block located near the axial center of the capsule.

The use of passive monitors such as those listed in Table 6-2 does not yield a direct measure of the energy-dependent neutron flux level at the point of interest. Rather, the activation or fission process is a measure of the integrated effect that the time and energy dependent neutron flux has on the target material over the course of the irradiation period. An accurate assessment of the average neutron flux level incident on the various monitors may be derived from the activation measurements only if the irradiation parameters are well known. In particular, the following variables are important:

- The operating history of the reactor
- The energy response of the monitor
- The neutron energy spectrum at the monitor location
- The physical characteristics of the monitor

The analysis of the passive monitors and the subsequent derivation of the average neutron flux require two operations. First, the disintegration rate of product nuclide per unit mass of monitor must be determined. Second, in order to define a suitable spectrum-averaged reaction cross section, the neutron energy spectrum at the monitor location must be calculated.

The specific activity of each monitors is determined using established ASTM procedures.[14-22] Following sample preparation, the activity of each monitor is determined by means of a lithium-drifted germanium, Ge(Li), gamma ray spectrometer. The overall standard deviation of the measured data is a function of the precision of sample weighing, the uncertainty in counting, and the acceptable error in detector calibration. For the samples removed from V. C. Summer Unit 1, the overall 2σ deviation in the measured data is determined to be plus or minus 10 percent. The neutron energy spectra at the monitor locations are determined analytically using the method described in Section 6-2.

Having the measured activity of the monitors and the neutron energy spectrum at the monitor locations of interest, the calculation of the neutron flux proceeds as follows.

The reaction product activity in the monitor is expressed as

$$A = N_o \, FY \int_E \sigma(E) \, \phi(E) \, dE \sum_{j=1}^{n} \frac{P_j}{P_{max}} C_j \left(1-e^{-\lambda t_j}\right) e^{-\lambda t_d} \qquad (6\text{-}1)$$

where

A = induced product activity (dps per gram)
N_o = number of target element atoms per gram
F = weight fraction of the target nuclide in the target material
Y = number of product atoms produced per reaction
$\sigma(E)$ = energy dependent reaction cross section

$\phi(E)$ = time averaged energy dependent neutron flux at the monitor location with the reactor at full (reference) power

P_j = average core power level during irradiation period j

P_{max} = maximum or reference core power level

λ = decay constant of the product nuclide

t_j = length of irradiation period j

t_d = decay time following irradiation period j

n = total number of irradiation periods

C_j = flux (E > 1.0 MeV) during irradiation period j divided by the average flux (E > 1.0 MeV) over the total irradiation. C_j is calculated with the adjoint neutron transport method and accounts for the change in neutron monitor response caused by core power distribution variations from fuel cycle to fuel cycle. P_j/P_{max}, which accounts for the month-by-month variation of power level within a fuel cycle, is applied to the full power based flux ratio, C_j.

Because the neutron flux distributions are calculated using multigroup transport methods and, further, because the main interest is in the fast (E > 1.0 MeV) neutron flux, spectrum averaged reaction cross sections are defined such that the integral term in Equation 6-1 is replaced by the following relation.

$$\int_E \sigma(E)\ \phi(E)\ dE = \sigma\phi_f$$

where:

$$\bar{\sigma} = \frac{\int_0^{\infty} \sigma(E)\ \phi(E)\ dE}{\int_0^{\infty} 1\ \text{MeV}\ \phi(E)\ dE} = \frac{\sum_{g=1}^{47} \sigma_g \phi_g}{\sum_{g=1}^{18} \phi_g}$$

$$\phi_f = \int_{1\ \text{MeV}}^{\infty} \phi(E)\ dE = \sum_{g=1}^{18} \phi_g$$

g = group number from Table 6-1.

Thus, Equation 6-1 is rewritten.

$$A = N_o F Y\ \phi f \sum_{j=1}^{n} \frac{P_j}{P_{max}} C_j \left(1 - e^{-\lambda t_j}\right) e^{-\lambda t_d}$$

or, solving for the fast (E > 1.0 MeV) neutron flux,

$$\phi_f = \frac{A}{N_o F Y\ \bar{\sigma} \sum_{j=1}^{n} \frac{P_j}{P_{max}} C_j \left(1 - e^{-\lambda t_j}\right) e^{-\lambda t_d}} \qquad (6\text{-}2)$$

The total fast (E > 1.0 MeV) neutron fluence is then given by

$$\Phi = \phi_f \sum_{j=1}^{n} \frac{P_j}{P_{max}} t_j \qquad (6\text{-}3)$$

where

$\sum_{j=1}^{n} \frac{P_j}{P_{max}} t_j$ = total effective full power seconds of reactor operation up to the time of capsule removal

An assessment of the potential for product nuclide burnout may be made using the bare and cadmium shielded cobalt measured activities and published data or the 2200 m/s absorption cross-section and the resonance integral. This is done by rewriting Equation 6-1 in terms of a monitor 2200 m/s neutron flux and a monitor resonance flux as follows:

$$A_{bare} = N_o FY \left(\sigma_{2200}\, \sigma_{2200} + RI\, \phi_{res}\right) \sum_{j=1}^{n} \frac{P_j}{P_{max}} C_j \left(1 - e^{-\lambda t_j}\right) e^{-\lambda t_d} \qquad (6\text{-}4)$$

$$A_{cd} = N_o FY \left(RI\, \phi_{res}\right) \sum_{j=1}^{n} \frac{P_j}{P_{max}} C_j \left(1 - e^{-\lambda t_j}\right) e^{-\lambda t_d} \qquad (6\text{-}5)$$

where

A_{bare} = bare induced product activity (dps per gram)

A_{cd} = cadmium shielded induced product activity (dps per gram)

σ_{2200} = published 2200 m/s absorption cross-section for nuclide of interest

RI = published epicadmium dilute resonance integral for nuclide of interest

ϕ_{2200} = monitor 2200 m/s neutron flux to be determined from measured activities

ϕ_{res} = monitor resonance neutron flux to be determined from measured activities

Equations 6-4 and 6-5 are solved for ϕ_{2200} and ϕ_{res} using the average measured bare and cadmium shielded cobalt activities at the monitor location.

The total loss rate of a product nuclide may then be expressed as the sum of its radioactive decay rate and the neutron absorption rate in that nuclide while the reactor is at power. The product nuclide neutron absorption rate may be estimated from the published data for σ_{2200} and RI and the smaller fluxes determined above. If the neutron absorption rate is small when compared to the decay rate then there is no concern regarding burnout.

6.4 NEUTRON TRANSPORT ANALYSIS RESULTS

Results of the discrete ordinates transport calculations for the V. C. Summer Unit 1 reactor are summarized in this section. Calculated fast (E > 1.0 MeV) neutron exposure results are presented in Tables 6-3 through 6-9. Date are presented at several azimuthal locations at the inner radius of the reactor vessel as well as at the center of each surveillance capsule.

Tables 6-3 through 6-7 list plant specific maximum fast neutron flux levels at 0°, 15°, 20°, 30°, and 45° at the reactor vessel inner radius for the first three fuel cycles, and projected to the expiration date (March 21, 2013) of the current operating license and a reference date of 32 EFPY. Plant specific beltline cumulative fluence levels for the three completed fuel cycles and design basis cumulative fluence levels based on a design basis 3 loop core power distribution (at the nominal plus 2 sigma level) are presented for each completed fuel cycle. Similar data for the center of the surveillance capsules located at 18.94 and 19.72 are given in Table 6-8 and 6-9, respectively. The measured fast neutron fluence for surveillance capsule U (withdrawn at the end of cycle 1) and surveillance capsule V (withdrawn at the end of cycle 3) is also presented in Table 6-9 for comparison with analytical results (see Section 6-5). The maximum neutron flux levels reflect a core axial power distribution peak to average ratio of 1.20.

It should be noted that implementation of a more severe low leakage pattern would act to reduce the projections of fluence at key locations. On the other hand, relaxation of the current low leakage

patterns or a return to out-in fuel management would increase those projections.

Table 6-10 provides the relative radial variation of fast neutron flux or fluence through the reactor vessel at zero and forty five degrees.

Figure 6-3 provides the relative axial variation of fast neutron flux and fluence over the beltline region of the reactor vessel. A three dimensional description of the fast neutron exposure of the reactor vessel wall can be constructed using the data given in Tables 6-4 through 6-10 and Figure 6-3 along with the relation.

$$\phi(R,\theta,Z) = \phi(\theta)\ F(R)\ G(Z)$$

where:

$\phi(R,\theta,Z)$ = fast neutron fluence at location R,θ,Z within the reactor vessel wall

$\phi(\theta)$ = fast neutron fluence at azimuthal location θ on the reactor vessel inner radius from Table 6-4 through 6-7

$F(R)$ = relative fast neutron flux at depth R into the reactor vessel from Table 6-10

$G(Z)$ = relative fast neutron flux at axial position Z from Figure 6-3

Analysis has shown that the radial and axial variations within the reactor vessel wall are relatively insensitive to the implementation of low leakage fuel management schemes. Thus, the above relationship provides a vehicle for a reasonable evaluation of fluence gradients within the reactor vessel wall.

In order to derive neutron flux and fluence levels from the measured disintegration rates, suitable spectrum-averaged reaction cross sections are required. The calculated neutron energy spectrum at the

center of the V. C. Summer surveillance capsules, listed in Table 6-12 was taken from the forward calculation. The resulting calculated spectrum-averaged cross sections for each of the five fast neutron reactions are given in Table 6-13.

6.5 INFLUENCE OF AN ENERGY DEPENDENT DAMAGE MODEL

The use of fast (E > 1 ^ MeV) neutron fluence to correlate measured material property changes to the neutron exposure of the materials for light water reactor applications has traditionally been accepted for development of damage trend curves as well as for implementation of trend curve data to assess reactor vessel condition. In recent years, however, it has been suggested that an exposure model that accounts for differences in neutron energy spectra between surveillance capsule location and positions within the reactor vessel wall could lead to a reduction in the uncertainties associated with damage trend curves as well as to a more accurate evaluation of damage gradients through the reactor vessel wall.

Because of this potential shift away from a threshold fluence towards an energy dependent damage function for data correlation, ASTM E-853, "Standard Practice Analysis and Interpretation of Light Water Reactor Surveillance Results", recommends reporting calculated displacements per iron atom (dpa) in addition to fast neutron fluence to provide a data base for future reference. The energy dependent dpa function to be used for this evaluation is specified in ASTM E-693, "Standard Practice for Characterizing Neutron Exposures in Ferritic Steels in Terms of Displacement per Atom (dpa)".

For the V. C. Summer Unit 1 reactor vessel, iron atom displacement rates at each surveillance capsule location and at positions within the reactor vessel wall have been calculated. The analysis has shown that for a given location the ratio of dpa/flux (E > 1.0 MeV) is insensitive to changing core power distribution. That is, while implementation of low leakage loading patterns significantly impact the magnitude and spatial distribution of the neutron field, changes in the relative neutron energy spectrum at a given location are

of second order. The dpa/flux (E > 1.0 MeV) ratios calculated for key locations in the V. C. Summer Unit 1 reactor geometry are given in Table 6-11. The data in Table 6-11 may be used on conjunction with the fast neutron fluence data provided in Section 6-4 to develop distributions of dpa within the surveillance capsules and the reactor vessel. Also provided in Table 6-11 are ratios of flux (E > 0.11 MeV) to flux (E > 1.0 MeV) calculated for key locations in the V. C. Summer reactor geometry.

6.6 NEUTRON DOSIMETRY RESULTS

The irradiation history of the V. C. Summer Unit 1 reactor is given in Tables 6-14 and 6-15 for surveillance capsules U and V respectively. The data were obtained from NUREG-0020.[23] All of the radiometric monitors are located at the radial center of the surveillance capsule.

Comparisons of measured and calculated saturated activity of the radiometric monitors contained in Capsule U and Capsule V are given in Tables 6-16 and 6-19 respectively. Note that the results presented for capsule U are an update of earlier work[24] based upon the current plant specific analysis.

The fast (E > 1.0 MeV) neutron flux and fluence levels derived for capsule U and capsule V using the spectrum averaged cross sections listed in Table 6-13 are given in Tables 6-17 and 6-20 respectively. Table 6-18 and 6-21 summarize the key nuclear data and results of the product nuclide burnout assessments that were performed for capsule U and capsule V. Due to the relatively low thermal and resonance neutron fluxes at the surveillance capsule location, the neutron absorption rate is negligibly small when compared to the radioactive decay rate. Therefore, no correction has been made for product nuclide burnout.

An examination of Table 6-17 shows that the average fast (E > 1.0 MeV) neutron flux derived from the five threshold reactions for capsule U is 1.795E+11 n/cm^2-sec with a 1σ standard deviation of ±6.6 percent. The calculated flux value of 1.692E+11 n/cm^2-sec based on the plant specific core power distribution is within six percent of the average value derived from the measurements.

An examination of Table 6-20 shows that the average fast (E > 1.0 MeV) neutron flux derived from the five threshold reactions for capsule V is 1.600E+11 n/cm^2-sec with a 1σ standard deviation of *8.9 percent. The calculated flux value 1.559E+11 n/cm^2-sec based on the plant specific core power distribution is within three percent of the average value derived from the measurements.

A summary of measured and calculated current fast neutron exposures for capsule V and for key reactor vessel locations is presented in Table 6-22. The measured value is given based on the average of all five threshold reactions listed in Table 6-20. End of life (EOL) reactor vessel fast neutron fluence projections are also included in Table 6-22.

Based on the data given in Table 6-20, the best estimate fast neutron exposure of Capsule V is

Φ = 1.47E+19 n/cm^2 (E > 1.0 MeV) at 2.93 EFPY.

Table 6-1

SAILOR 47 Neutron Energy Group Structure

Energy Group	Group Lower Energy (MeV)	Energy Group	Group Lower Energy (MeV)
1	14.19[a]	25	0.183
2	12.21	26	0.111
3	10.00	27	0.0674
4	8.61	28	0.0409
5	7.41	29	0.0318
6	6.07	30	0.0261
7	4.97	31	0.0242
8	3.68	32	0.0219
9	3.01	33	0.0150
10	2.73	34	7.10E-3
11	2.47	35	3.36E-3
12	2.37	36	1.59E-3
13	2.35	37	4.54E-4
14	2.23	38	2.14E-4
15	1.92	39	1.01E-4
16	1.65	40	3.73E-5
17	1.35	41	1.07E-5
18	1.00	42	5.04E-6
19	0.821	43	1.86E-6
20	0.743	44	8.76E-7
21	0.608	45	4.14E-7
22	0.498	46	1.00E-7
23	0.369	47	0.00
24	0.298		

[a] The upper energy of group 1 is 17.33 MeV.

Table 6-2

Nuclear Constants for Radiometric Monitors Contained in the V. C. Summer Unit 1 Surveillance Capsules

Monitor Materials	Reaction of Interest	Target Weight Fraction	Product Half-life	Fission Yield (%)
Iron wire	Fe^{54} (n,p) Mn^{54}	0.058	312.2 dy	
Nickel wire	Ni^{58} (n,p) Co^{58}	0.6827	70.91 dy	
Copper wire	Cu^{63} (n,a) Co^{60}	0.6917	5.272 yr	
Uranium-238 in U_3O_8 [a]	U^{238} (n,f) Cs^{137}	1.0	30.17 yr	6.0
Neptunium-237 in NpO_2 [a]	Np^{237} (n,f) Cs^{137}	1.0	30.17 yr	6.5
Cobalt-aluminum wire [a]	Co^{59} (n,γ) Co^{60}	0.0015	5.272 yr	
Cobalt-aluminum wire	Co^{59} (n,γ) Co^{60}	0.0015	5.272 yr	

[a] Denotes that the monitor is cadmium-shielded.

Table 6-3

Fast (E > 1.0 MeV) Neutron Exposure at the Reactor Vessel Inner Radius - Azimuthal Angle of 0°

Cycle No.	Irradiation Time (EFPS)	Cycle Average Flux (n/cm^2-sec)	Beltline Region Cumulative Fluence (n/cm^2) Plant Specific	Beltline Region Cumulative Fluence (n/cm^2) Design Basis[a]	Cumulative Time (EFPY)
1	3.567E+07	5.55E+10	1.98E+18	2.35E+18	1.13
2	2.115E+07	4.28E+10	2.88E+18	3.75E+18	1.80
3[b]	3.550E+07	4.22E+10	4.38E+18	6.10E+18	2.93
EOL 2013[c]	7.799E+08	4.25E+10[d]	3.32E+19	5.76E+19	26.51
EOL 2022	1.052E+09	4.25E+10[d]	4.47E+19	1.27E+20	35.14

[a] Design Basis Flux: 6.60E+10 n/cm^2-sec

[b] End of Cycle 3 (Shutdown): March 6, 1987

[c] Present Operating License Expires: March 21, 2013

[d] Time Weighted Average Neutron Flux for Projections

Table 6-4

Fast (E > 1.0 MeV) Neutron Exposure at the Reactor Vessel Inner Radius - Azimuthal Angle of 15°

Cycle No.	Irradiation Time (EFPS)	Cycle Average Flux (n/cm^2-sec)	Beltline Region Cumulative Fluence (n/cm^2) Plant Specific	Design Basis[a]	Cumulative Time (EFPY)
1	3.567E+07	3.62E+10	1.29E+18	1.58E+18	1.13
2	2.115E+07	3.04E+10	1.93E+18	2.53E+18	1.80
3[b]	3.550E+07	2.99E+10	3.00E+18	4.11E+18	2.93
EOL 2012[c]	7.799E+08	3.01E+10[d]	2.35E+19	3.88E+19	26.51
EOL 2022	1.052E+09	3.01E+10[d]	3.16E+19	8.57E+19	35.41

[a] Design Basis Flux: 4.45E+10 n/cm^2-sec

[b] End of Cycle 3 (Shutdown): March 6, 1987

[c] Present Operating License Expires: March 21, 2013

[d] Time Weighted Average Neutron Flux for Projections

Table 6-5

Fast (E > 1.0 MeV) Neutron Exposure at the Reactor Vessel Inner Radius - Azimuthal Angle of 20°

Cycle No.	Irradiation Time (EFPS)	Cycle Average Flux (n/cm^2-sec)	Beltline Region Cumulative Fluence (n/cm^2) Plant Specific	Beltline Region Cumulative Fluence (n/cm^2) Design Basis[a]	Cumulative Time (EFPY)
1	3.567E+07	3.04E+10	1.08E+18	1.35E+18	1.13
2	2.115E+07	2.87E+10	1.69E+18	2.15E+18	1.80
3[b]	3.550E+07	2.66E+10	2.64E+18	3.49E+18	2.93
EOL 2013[c]	7.799E+08	2.74E+10[d]	2.14E+19	3.30E+19	26.51
EOL 2022	1.052E+09	2.74E+10[d]	2.88E+19	7.28E+19	35.14

[a] Design Basis Flux: 3.78E+10 n/cm^2-sec

[b] End of Cycle 3 (Shutdown): March 6, 1987

[c] Present Operating License Expires: March 21, 2013

[d] Time Weighted Average Neutron Flux for Projections

Table 6-6

Fast (E > 1.0 MeV) Neutron Exposure at the Reactor Vessel Inner Radius--Azimuthal Angle of 30°

Cycle No.	Irradiation Time (EFPS)	Cycle Average Flux (n/cm^2-sec)	Beltline Region Cumulative Fluence (n/cm^2) Plant Specific	Beltline Region Cumulative Fluence (n/cm^2) Design Basis[a]	Cumulative Time (EFPY)
1	3.567E+07	2.39E+10	8.55E+17	1.04E+18	1.13
2	2.115E+07	2.18E+10	1.31E+18	1.65E+18	1.80
3[b]	3.550E+07	2.00E+10	2.02E+18	2.69E+18	2.93
EOL 2013[c]	7.799E+08	2.07E+10[d]	1.61E+19	2.54E+19	26.51
EOI 2022	1.052E+09	2.07E+10[d]	2.17E+19	5.61E+19	35.14

[a] Design Basis Flux: 2.912E+10 n/cm^2-sec

[b] End of Cycle 3 (Shutdown): March 6, 1987

[c] Present Operating License Expires: March 21, 2013

[d] Time Weighted Average Neutron Flux for Projections

Table 6-7

Fast (E > 1.0 MeV) Neutron Exposure at the Reactor Vessel Inner Radius--Azimuthal Angle of 45°

Cycle No.	Irradiation Time (EFPS)	Cycle Average Flux (n/cm^2-sec)	Beltline Region Cumulative Fluence (n/cm^2) Plant Specific	Beltline Region Cumulative Fluence (n/cm^2) Design Basis[a]	Cumulative Time (EFPY)
1	3.567E+07	1.71E+10	6.10E+17	7.40E+17	1.13
2	2.115E+07	1.35E+10	8.96E+17	1.17E+18	1.80
3[b]	3.550E+07	1.35E+10	1.37E+18	1.91E+18	2.93
EOL 2013[c]	7.799E+08	1.35E+10[d]	1.05E+18	1.81E+19	26.51
EOL 2022	1.052E+09	1.35E+10[d]	1.42E+19	3.99E+19	35.14

[a] Design Basis Flux: 2.078E+10 n/cm^2-sec

[b] End of Cycle 3 (Shutdown): March 6, 1987

[c] Present Operating License Expires: March 21, 2013

[d] Time Weighted Average Neutron Flux for Projections

Table 6-8

Fast (E > 1.0 MeV) Neutron Exposure at the 16.94 Degree Surveillance Capsule Center

Cycle No.	Irradiation Time (EFPS)	Cycle Average Flux (n/cm^2-sec)	Beltline Region Cumulative Fluence (n/cm^2) Plant Specific	Design Basis[a]	Capsule Data (n/cm^2)
1	3.567E+07	1.69E+11	6.03E+18	7.45E+18	6.39E+18:U
2	2.115E+07	1.52E+11	9.26E+18	1.18E+19	
3[b]	3.550E+07	1.46E+11	1.44E+19	1.92E+19	1.47E+19:V
EOL 2013[c]	7.799E+08	1.48E+11[d]	1.16E+20	1.82E+20	
EOL 2022	1.052E+09	1.48E+11[d]	1.56E+20	4.02E+20	

[a] Design Basis Flux: 2.09E+11 n/cm^2-sec

[b] End of Cycle 3 (Shutdown): March 6, 1987

[c] Present Operating License Expires: March 21, 2013

[d] Time Weighted Average Neutron Flux for Projections

Table 6-9

Fast (E > 1.0 MeV) Neutron Exposure at the 19.72 Degree Surveillance Capsule Center

Cycle No.	Irradiation Time (EFPS)	Cycle Average Flux (n/cm^2-sec)	Beltline Region Cumulative Fluence (n/cm^2) Plant Specific	Beltline Region Cumulative Fluence (n/cm^2) Design Basis[a]	Cumulative Time (EFPY)
1	3.567E+07	1.46E+11	5.21E+18	6.44E+18	1.13
2	2.115E+07	1.38E+11	8.14E+18	1.02E+19	1.80
3[b]	3.550E+07	1.28E+11	1.26E+19	1.66E+19	2.93
EOL 2013[c]	7.799E+08	1.32E+11[d]	1.02E+20	1.57E+20	26.51
EOL 2022	)52E+09	1.32E+11	1.38E+20	4.02E+20	35.14

[a] Design Basis Flux: 1.81E+11 n/cm^2-sec

[b] End of Cycle 3 (Shutdown): March 6, 1987

[c] Present Operating License Expires: March 21, 2013

[d] Time Weighted Average Neutron Flux for Projections

Table 6-10

Calculated Relative Fast Neutron Exposure Parameters
for V. C. Summer Unit 1

Relative Radial Variation of Fast (E > 1.0 MeV)
Neutron Flux or Fluence Through the Reactor Vessel

Radial Location	Radius (cm)	Azimuthal Angle	
		0 Degrees	45 Degrees
IR	199.390	1.0	1.0
1/4 T	204.390	0.592	0.601
1/2 T	209.391	0.294	0.305
3/4 T	214.392	0.138	0.147
OR	219.392	0.0567	0.0669

Table 6-11

Ratios of Fast Neutron Exposure Parameters to Fast (E > 1.0 MeV) Neutron Flux for the Reactor Vessel and Surveillance Capsules

Location	Fast (E > 1.0 MeV) Neutron Flux Ratio		Iron Displacement Rate (dps/sec) Ratio	
	0 Deg.	45 Deg.	0 Deg.	45 Deg.
RV IR	2.42	1.94	1.59E-21	1.55E-21
RV 1/4 T	3.61	2.96	1.82E-21	1.70E-21
RV 1/2 T	5.30	4.51	2.27E-21	2.13E-21
RV 3/4 T	7.38	6.02	2.85E-21	2.44E-21
RV OR	9.10	8.23	3.37E-21	3.20E-21
17° Capsule	5.00		2.136E-21	
20° Capsule	4.86		2.099E-21	

Units: $\frac{n/cm^2\text{-sec } (E > 0.1 \text{ MeV})}{n/cm^2\text{-sec } (E > 1.0 \text{ MeV})}$ $\frac{dps/sec}{n/cm^2\text{-sec } (E > 1.0 \text{ MeV})}$

Table 6-12

Calculated Neutron Energy Spectra at the Center of the V. C. Summer Unit 1 Surveillance Capsule V

Energy Group	Neutron Flux (n/cm^2-sec)	Energy Group	Neutron Flux (n/cm^2-sec)
1	3.00E+07	25	1.29E+11
2	1.11E+08	26	1.42E+11
3	3.89E+08	27	1.18E+11
4	7.17E+08	28	7.38E+10
5	1.21E+09	29	1.96E+10
6	2.71E+09	30	1.04E+10
7	3.80E+09	31	3.16E+10
8	7.95E+09	32	2.25E+10
9	7.46E+09	33	2.96E+10
10	6.27E+09	34	3.63E+10
11	7.61E+09	35	6.65E+10
12	3.81E+09	36	6.74E+10
13	1.16E+09	37	9.04E+10
14	5.90E+09	38	4.54E+10
15	1.64E+10	39	5.04E+10
16	2.25E+10	40	6.95E+10
17	3.60E+10	41	8.04E+10
18	8.62E+10	42	4.26E+10
19	6.58E+10	43	4.37E+10
20	3.06E+10	44	2.41E+10
21	1.21E+11	45	1.61E+10
22	9.51E+10	46	1.68E+10
23	1.28E+11	47	1.68E+10
24	1.29E+11		

Table 6-13

Spectrum Averaged Reaction Cross Section At the Center of the V. C. Summer Unit 1 Surveillance Capsules

Reaction of Interest	Spectrum-Average Cross Section[a] (barns)
Fe^{54} (n,p) Mn^{54}	0.0515
Ni^{58} (n,p) Co^{58}	0.0726
Cu^{63} (n,α) Co^{60}	0.000428
U^{238} (n,f) Cs^{137}	0.301
Np^{237} (n,f) Cs^{137}	3.43

(a) $$\bar{\sigma} = \frac{\int_0^{\infty} \sigma(E)\, \phi(E)\, dE}{\int_{1\ MeV}^{\infty} \sigma(E)\, dE}$$

Table 6-14

V. C. Summer Unit 1 Power History, Capsule U from NUREG-0020

Reactor (MWT) 2775
NSSS Power (MWT) 2785

Cycle 1

Date		Gross Thermal Energy (MWH)	
m	y	Monthly	Lifetime
11	82	143789	143789
12	82	651071	794860
1	83	975351	1770211
2	83	844552	2614763
3	83	566778	3181541
4	83	0	3181541
5	83	265111	3446652
6	83	1673672	5120324
7	83	1863508	6983832
8	83	1758090	8741922
9	83	1749405	10491327
10	83	1810240	12301567
11	83	1518120	13819687
12	83	800616	14620303
1	84	1996935	16617238
2	84	1666309	18283547
3	84	1459743	19743290
4	84	119028	19862318
5	84	1704230	21566548
6	84	1847339	23413887
7	84	833316	24247203
8	84	1844750	26091953
9	84	1405054	27497007

Cycle 1 parameters
Startup: Nov. 15, 1982
Shutdown: Sept. 28, 1984

EFPY = 1.13
EFPS = 3.567E+07

Capsule U Removed

Table 6-15

V. C. Summer Unit 1 Power History, Capsule V from NUREG-0020

Reactor (MWT) 2775
NSSS Power (MWT) 2785

Cycle 1

Date		Gross Thermal Energy (MWH)	
m	y	Monthly	Lifetime
11	82	143789	143789
12	82	651071	794860
1	83	975351	1770211
2	83	844552	2614763
3	83	566778	3181541
4	83	0	3181541
5	83	265111	3446652
6	83	1673672	5120324
7	83	1863508	6983832
8	83	1758090	8741922
9	83	1749405	10491327
10	83	1810240	12301567
11	83	1518120	13819687
12	83	800616	14620303
1	84	1996935	16617238
2	84	1666309	18283547
3	84	1459743	19743290
4	84	119028	19862318
5	84	1704230	21566548
6	84	1847339	23413887
7	84	833316	24247203
8	84	1844750	26092953
9	84	1405054	27497007

Cycle 1 Parameters
Startup: Nov. 16, 1982
Shutdown: Sept. 28, 1984

EFPY = 1.13
EFPS = 3.567E+07

Table 6-15 (cont'd.)

Cycle 2

Date		Gross Thermal Energy (MWH)	
m	y	Monthly	Lifetime
12	84	455882	27952889
1	85	1515633	29468522
2	85	1578286	31046808
3	85	1896308	32943116
4	85	1682110	34625226
5	85	1256696	35881922
6	85	1989561	37871483
7	85	2053141	39924624
8	85	1742390	41667014
9	85	1836663	43503677
10	85	292854	43796531

Cycle 2 Parameters
Startup: Dec. 19, 1984
Shutdown: Oct. 5, 1985

EFPY = 1.80
EFPS = 2.11E+07

Table 6-15 (cont'd.)

Cycle 3

Date		Gross Thermal Energy (MWH)	
m	y	Monthly	Lifetime
12	85	661338	44457869
1	86	2039156	46497025
2	86	1638382	48135407
3	86	2061270	50196677
4	86	1898100	52094777
5	86	2021310	54116087
6	86	1461204	55577291
7	86	1898812	57476103
8	86	2037220	59513323
9	86	1957929	61471252
10	86	1835749	63307001
11	86	1862802	65169803
12	86	1844820	67014623
1	87	1977210	68991833
2	87	1838160	70829993
3	87	333666	71163659

Cycle 3 Parameters
Startup: Dec. 16, 1985
Shutdown: March 6, 1987

EFPY = 2.93
EFPS = 3.55E+07

Capsule V removed

Table 6-16

Comparison of Measured and Calculated Radiometric Monitor Saturated Activities for V. C. Summer Unit 1 Surveillance Capsule U

Monitor and Axial Location[a]	Radiometric Monitor Saturated Activity (Disintegrations/Second-Gram) Measured		Basis	Calculated	C/M
$Fe^{54}(n,p)Mn^{54}$			(gm of wire)		
Top	5.514E+6				
Middle	5.460E+6				
Bottom	5.929E+6				
Average[b]	5.634E+6	[±4.6%]		5.652E+6	1.003
$Ni^{58}(n,p)Co^{58}$			(gm of wire)		
Top	9.173E+7				
Middle	8.674E+7				
Bottom	9.363E+7				
Average[b]	9.070E+7	[±3.9%]		8.726E+7	0.962
$Cu^{63}(n,\alpha)Co^{60}$			(gm of wire)		
Top	5.568E+5				
Middle	5.491E+5				
Bottom	5.728E+5				
Average[b]	5.596E+5	[±2.2%]		4.798E+5	0.857
$U^{238}(n,f)Cs^{137}$[c]			(gm of wire)		
Middle	1.010E+7				
Corrected[d]	8.059E+6			7.750E+6	0.962
$Np^{237}(n,f)Cs^{137}$[c]			(gm of wire)		
Middle	9.489E+7			9.616E+7	1.013

Table 6-16 (cont'd)

Monitor and Axial Location[a]	Radiometric Monitor Saturated Activity (Disintegrations/Second-Gram) Measured	Basis	Calculated	C/M
$Co^{59}(n,\gamma)Co^{60}$(c)		(gm of wire)		
Top	6.800E+7			
Middle	6.922E+7			
Bottom	7.028E+7			
Average[b]	6.917E+7 [±1.6%]		5.911E+7	0.855
$Co^{59}(n,\gamma)Co^{60}$		(gm of wire)		
Top	1.235E+8			
Middle	1.269E+8			
Bottom	1.268E+8			
Average[b]	1.257E+8 [±1.6%]		6.936E+7	0.552

(a) Refer to Figure 4-2 for the location of the various radiometric monitors.

(b) The standard deviation (1σ) of the mean saturated activity is expressed as a percentage of the mean.

(c) This radiometric monitor was cadmium shielded.

(d) The measured value has been multiplied by 0.798 to correct for the effect of 323 ppm U^{235} and the build up of Pu^{239}.

Table 6-17

Results of Fast Neutron Dosimetry for V. C. Summer Unit 1
Surveillance Capsule U

Reaction of Interest	Radiometric Monitor Saturated Activity[a] (dps/gm)		Fast (E > 1.0 MeV) Neutron Flux (n/cm^2-sec)		Current[b] Fast E > 1.0 MeV) Neutron Fluence (n/cm^2)	
	Measured	Calculated	Measured	Calculated	Measured	Calculated
$Fe^{54}(n,p)Mn^{54}$	5.634E+6	5.652E+6	1.749E+11		6.240E+18	
$Ni^{58}(n,p)Co^{58}$	9.070E+7	8.726E+7	1 783E+11		6.362E+18	
$Cu^{63}(n,\alpha)Co^{60}$	5.596E+5	4.798E+5	1.995E+11		7.115E+18	
$U^{238}(n,f)Cs^{137}$	8.059E+6	7.750E+6	1.776E+11		6.301E+18	
$Np^{237}(n,f)Cs^{137}$	9.489E+7	9.616E+7	1.675E+11		5.976E+18	
Average			1.795E+11 [*6.65]	1.692E+11	6.398E+18	6.034E+18

[a] Refer to Table 6-16.

[b] Total irradiation time for surveillance Capsule U is 3.567E+07 effective full power second (EFPS).

Table 6-18

Product Nuclide Burnout Assessment for V. C. Summer Unit 1 Surveillance Capsule U

Nuclear Data

Nuclide	Half-Life	2200 (barns)	RI (barns)
Mn^{54}	312.2 dy	10.0	-
Co^{58}	70.91 dy	1880	6890
Co^{59}	Stable	37.2	75.5
Co^{60}	5.272 yr	2.0	4.3
Cs^{137}	30.17 yr	0.11	0.50

Surveillance Capsule U Averaged Saturated Co^{60} Activity

Bare Co-Al Wire: A = 1.26E+08 dps/gm

Cd Shielded Co-Al Wire: A = 6.92E+07 dps/gm

Monitor Fluxes Derived From Co^{60} Saturated Activity

ϕ(2200) = 9.92E+10 n/cm^2-sec

ϕ(RES) = 5.98E+10 n/cm^2-sec

Product Nuclide Loss Rate Comparison

Nuclide	Decay Constant (1/sec)	Absorption Rate (1/sec)
Mn^{54}	2.57E-08	9.92E-13
Co^{58}	1.13E-07	5.98E-10
Co^{60}	4.17E-09	4.55E-13
Cs^{137}	7.28E-10	2.99E-14

Table 6-19

Comparison of Measured and Calculated Radiometric Monitor Saturated Activities for V. C. Summer Unit 1 Surveillance Capsule V

Monitor and Axial Location[a]	Radiometric Monitor Saturated Activity (Disintegrations/Second-Gram Measured		Basis	Calculated	C/M
$Fe^{54}(n,p)Mn^{54}$			(gm of wire)		
Top	5.177E+6				
Middle	5.351E+6				
Bottom	5.056E+6				
Average[b]	5.195E+6	[±2.9%]		5.235E+6	1.008
$Ni^{58}(n,p)Co^{58}$			(gm of wire)		
Top	7.939E+7				
Middle	8.084E+7				
Bottom	7.615E+7				
Average[b]	7.879E+7	[±3.0%]		8.082E+7	1.026
$Cu^{63}(n,\alpha)Co^{60}$			(gm of wire)		
Top	5.098E+5				
Middle	5.237E+5				
Bottom	5.098E+5				
Average[b]	5.144E+5	[±1.6%]		4.444E+5	0.864
$U^{238}(n,f)Cs^{137}$[c]			(gm of wire)		
Middle	9.540E+6				
Corrected[d]	7.090E+6			7.178E+6	1.012
$Np^{237}(n,f)Cs^{137}$[c]			(gm of wire)		
Middle	8.226E+7			8.907E+7	1.083

Table 6-19 (cont'd)

Monitor and Axial Location[a]	Radiometric Monitor Saturated Activity (Disintegrations/Second-Gram) Measured		Basis	Calculated	C/M
$Co^{59}(n,\gamma)Co^{60}$[c]			(gm of wire)		
Top	7.040E+7				
Middle	6.381E+7				
Bottom	6.381E+7				
Average[b]	6.601E+7	[±5.8%]		5.475E+7	0.829
$Co^{59}(n,\gamma)Co^{60}$			(gm of wire)		
Top	1.120E+8				
Middle	1.169E+8				
Bottom	1.155E+8				
Average[b]	1.148E+8	[±2.2%]		6.424E+7	0.560

(a) Refer to Figure 4-2 for the location of the various radiometric monitors.

(b) The standard deviation (1σ) of the mean saturated activity is expressed as a percentage of the mean.

(c) This radiometric monitor was cadmium shielded.

(d) The measured value has been multiplied by 0.743 to correct for the effect of 232 pm U^{235} and the build up of Pu^{239}.

Table 6-20

Results of Fast Neutron Dosimetry for V. C. Summer
Unit 1 Surveillance Capsule V

Reaction of Interest	Radiometric Monitor Saturated Activity[a] (dps/gm)		Fast (E > 1.0 MeV) Neutron Flux (n/cm^2-sec)		Current[b] Fast (E > 1.0 MeV) Neutron Fluence (n/cm^2)	
	Measured	Calculated	Measured	Calculated	Measured	Calculated
$Fe^{54}(n,p)Mn^{54}$	5.195E+6	5.235E+6	1.613E+11		1.489E+19	
$Ni^{58}(n,p)Co^{58}$	7.879E+7	8.082E+7	1.549E+11		1.430E+19	
$Cu^{63}(n,\alpha)Co^{60}$	5.144E+5	4.444E+5	1.834E+11		1.693E+19	
$U^{238}(n,f)Cs^{137}$	7.088E+6	7.178E+6	1.554E+11		1.435E+19	
$Np^{237}(n,f)Cs^{137}$	8.226E+7	8.907E+7	1.452E+11		1.341E+19	
Average			1.600E+11 [±8.9%]	1.559E+11	1.477E+19	1.44E+19

[a] Refer to Table 6-19.

[b] Total irradiation time for surveillance Capsule V is 9.232E+07 effective full power second (EFPS).

Table 6-21

Product Nuclide Burnout Assessment for V. C. Summer Unit 1
Surveillance Capsule V

Nuclear Data

Nuclide	Half-Life	2200 (barns)	RI (barns)
Mn^{54}	312.2 dy	10.0	-
Co^{58}	70.91 dy	1880	6890
Co^{59}	Stable	37.2	75.5
Co^{60}	5.272 yr	2.0	4.3
Cs^{137}	30.17 yr	0.11	0.50

Surveillance Capsule V Average Saturated Co^{60} Activity

Bare Co-Al Wire: A = 1.15E+08 dps/gm

Cd Shielded Co-Al Wire: A=6.60E+07 dps/gm

Monitor Fluxes Derived from Co^{60} Saturated Activity

ϕ(2200) = 8.56E+10 $n/cm^2/sec$

ϕ(RES) = 5.70E+10 $n/cm^2/sec$

Product Nuclide Loss Rate Comparison

Nuclide	Decay Constant (1/sec)	Absorption Rate (1/sec)
Mn^{54}	2.57E-08	8.56E-13
Co^{58}	1.13E-07	5.54E-10
Co^{60}	4.17E-09	4.16E-13
Cs^{137}	7.28E-10	2.85E-14

Table 6-22

Summary of V. C. Summer Unit 1 Fast Neutron Fluence Results
Based on Surveillance Capsule V

Location	Current Fast (E > 1.0 MeV) Neutron Fluence n/cm^2		End of Life Fast (E > 1.0 MeV) Neutron Fluence) n/cm^2	
	Measured	Calculated	Measured	Calculated
Capsule V	1.47E+19	1.44E+19		
Vessel IR	4.72E+18	4.63E+18	6.73E+19	6.60E+19
Vessel 1/4 T	2.80E+18	2.75E+18	3.99E+19	3.92E+19
Vessel 3/4 T	6.50E+17	6.37E+17	9.27E+18	9.08E+18

(a) Current fluences are based on operation at 2775 MWt for 2.93 EFPY.

(b) EOL fluences are based on operation at 2775 MWt for 32 EFPY.

(c) The measured results of surveillance Capsule V were extrapolated to the reactor vessel locations using the following-calculated lead factors:

Inner Radius - 3.11
1/4 Thickness - 5.24
3/4 Thickness - 22.6

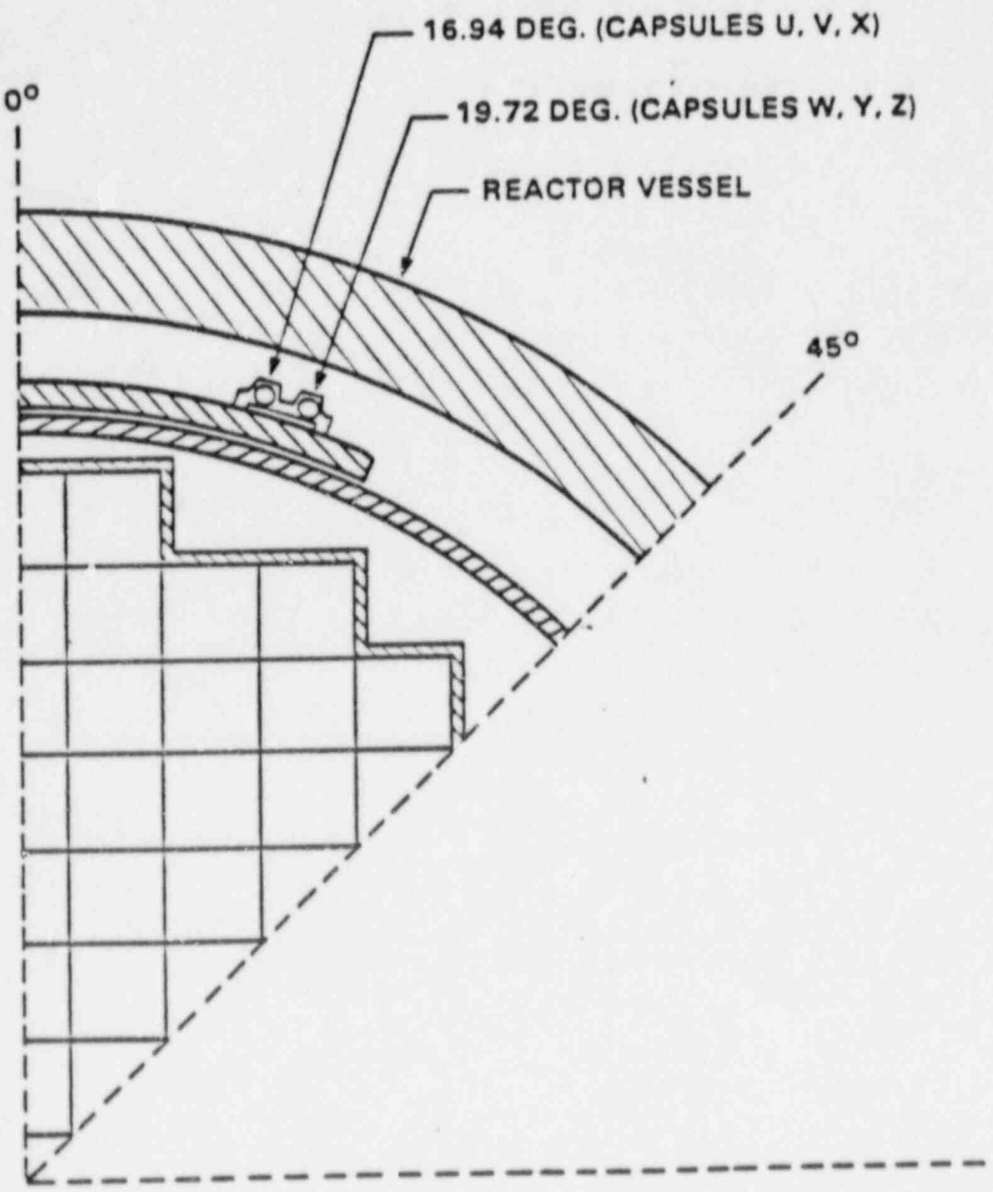

Figure 6-1. V. C. Summer Unit 1 reactor geometry

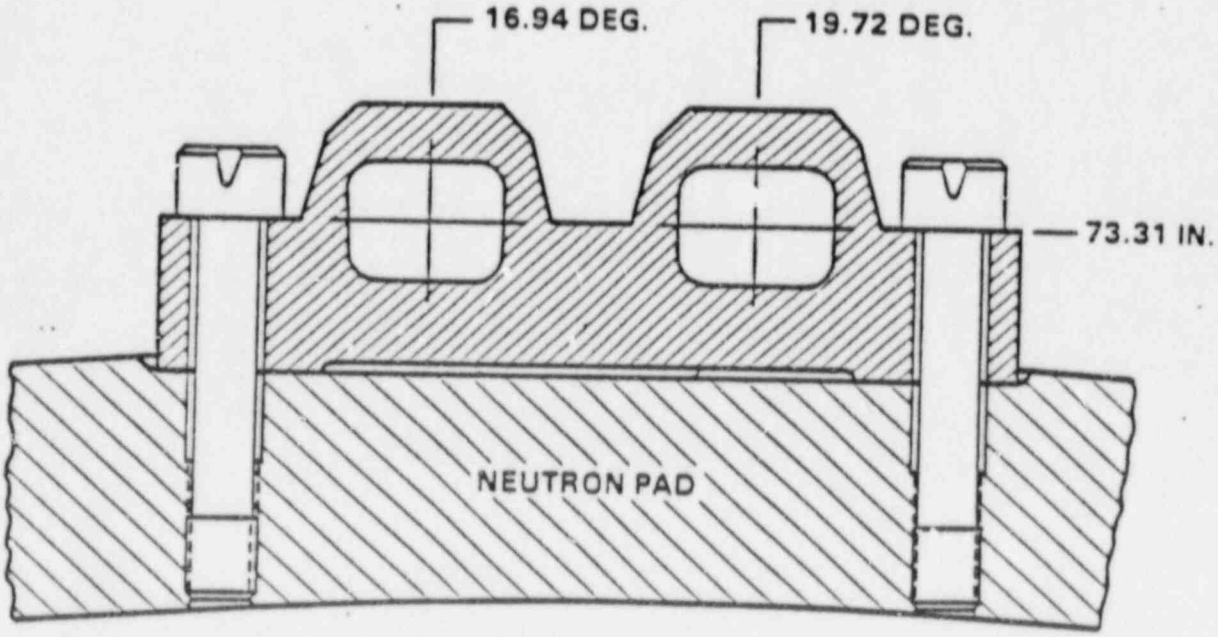

Figure 6-2. Plan view of a dual reactor vessel surveillance capsule

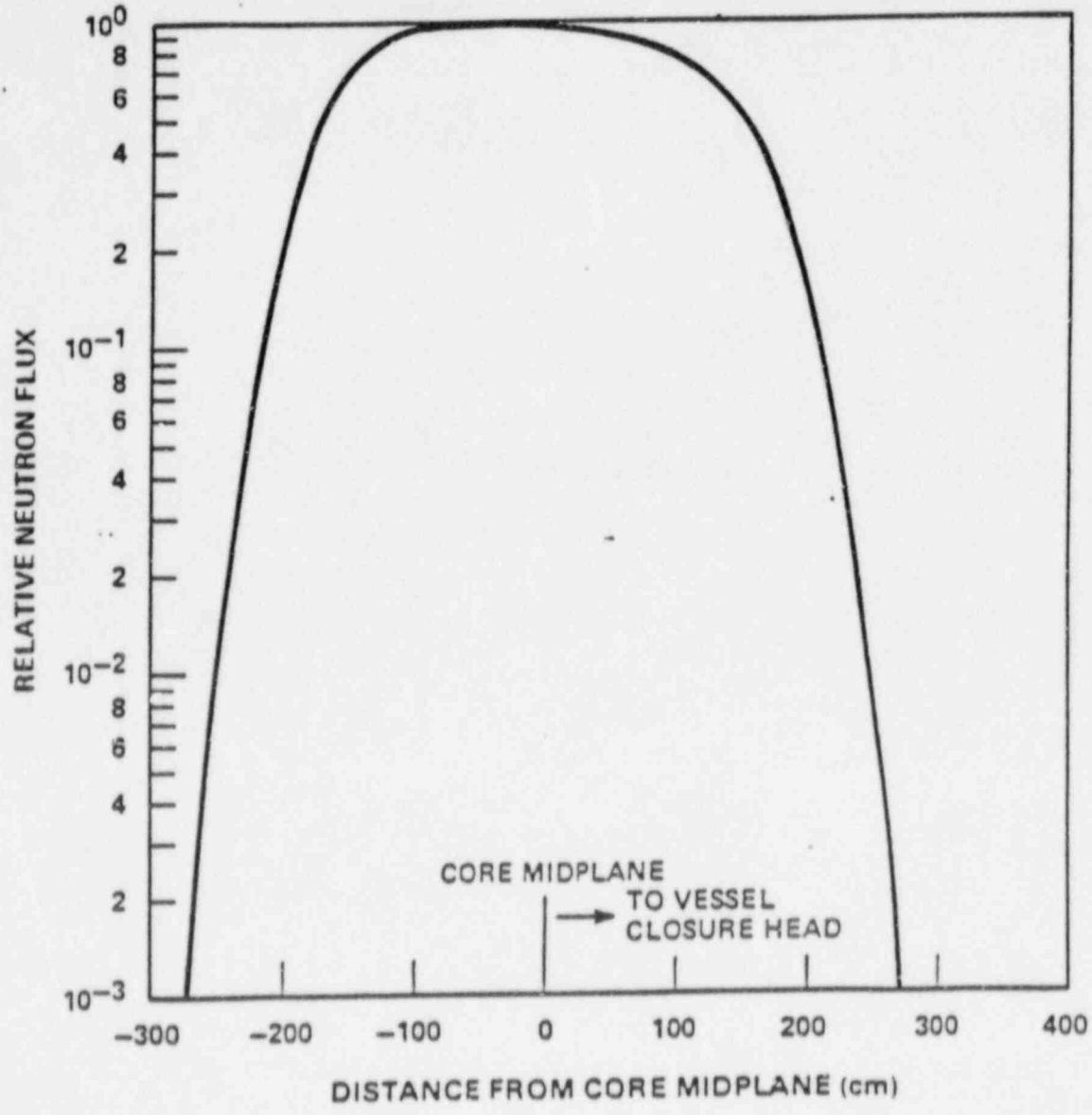

Figure 6-3. Relative axial variation of fast (E > 1.0 MeV) neutron flux within the reactor vessel wall

7. SURVEILLANCE CAPSULE REMOVAL SCHEDULE

The following removal schedule is based on ASTM E185-82 and is recommended for future capsules to be removed from the V. C. Summer Unit 1 reactor vessel:

Capsule	Vessel Location (deg.)	Lead Factor	Removal Time[a]	Estimated Fluence (n/cm^2)
U	343	3.11	1.13 (Removed)	6.39×10^{18}
V	107	3.11	2.93 (Removed)	1.47×10^{19}
X	287	3.11	6	3.85×10^{19}[b]
W	110	2.69	12	6.65×10^{19}[c]
Y	290	2.69	20	11.10×10^{19}
Z	340	2.69	Standby	-

---

[a] Effective full power years from plant startup.

[b] Approximate fluence at 1/4 thickness reactor vessel wall at end of life.

[c] Approximate fluence at reactor vessel inner wall at end of life.

8. REFERENCES

1. J. A. Davidson and S. E. Yanichko, "South Carolina Electric and Gas Company, V. C. Summer Nuclear Plant Unit No. 1 Reactor Vessel Radiation Surveillance Program", WCAP-9234, January 1978.

2. Code of Federal Regulations, 10CFR50, Appendix G, "Fracture Toughness Requirements", and Appendix H, "Reactor Vessel Material Surveillance Program Requirements", U.S. Nuclear Regulatory Commission, Washington, D.C.

3. Regulatory Guide 1.99, Proposed Revision 2, "Radiation Damage to Reactor Vessel Materials", U.S. Nuclear Regulatory Commission, February, 1986.

4. R. G. Soltesz, R. K. Disney, J. Jedruch, and S. L. Ziegler, "Nuclear Rocket Shielding Methods, Modification, Updating and Input Data Preparation. Vol. 5--Two-Dimensional Discrete Ordinates Transport Technique", WANL-PR(LL)-034, Vol 5, August 1970.

5. "ORNL RSIC Data Library Collection DLC-76, SAILOR Coupled Self-Shielded, 47 Neutron, 20 Gamma-Ray, P3, Cross Section Library for Light Water Reactors".

6. S. L. Anderson and K. C. Tran, WCAP-11428, "Benchmark Testing of Westinghouse Neutron Transport Analysis Methodology _ PCA Evaluations", April 1987.

7. A. H. Fero, WCAP-11173 (NUREG/CR-4827), "Neutron and Gamma-Ray Flux Calculations for the Venus PWR Engineering Mockup", January 1987.

8. Benchmark Testing of Westinghouse Neutron Transport Analysis Methodology - Surveillance Capsule Data Base (to be published).

9. ASTM Designation E482-82, "Standard Guide for Application of Neutron Transport Methods for Reactor Vessel Surveillance", in ASTM Standards, Section 12, American Society for Testing and Materials, Philadelphia, PA, 1986.

10. ASTM Designation E560-84, "Standard Practice for Extrapolating Reactor Vessel Surveillance Dosimetry Results", in ASTM Standards, Section 12, American Society for Testing and Materials, Philadelphia, PA, 1986.

11. ASTM Designation E693-79 (Reapproved 1985), "Standard Practice for Characterizing Neutron Exposures in Ferritic Steels in Terms of Displacements per Atom (dpa)", in ASTM Standards, Section 12, American Society for Testing Materials, Philadelphia, PA, 1986.

12. ASTM Designation E706-84, "Standard Master Matrix for Light-Water Reactor Pressure Vessel Surveillance Standards", in ASTM Standards, Section 12, American Society for Testing and Materials, Philadelphia, PA, 1986.

13. ASTM Designation E853-84, "Standard Practice for Analysis and Interpretation of Light-Water Reactor Surveillance Results", in ASTM Standards, Section 12, American Society for Testing and Materials, Philadelphia, PA, 1986.

14. ASTM Designation E261-77, "Standard Method for Determining Neutron Flux, Fluence, and Spectra by Radioactivation Techniques", in ASTM Standards, Section 12, American Society for Testing and Materials, Philadelphia, PA, 1986.

15. ASTM Designation E262-85, "Standard Method for Determining Thermal Neutron Reaction and Fluence Rates by Radioactivation Techniques", in ASTM Standards, Section 12, American Society for Testing and Materials, Philadelphia, PA, 1986.

16. ASTM Designation E263-82, "Standard Method for Determining Fast-Neutron Flux Density by Radioactivation of Iron", in ASTM Standards, Section 12, American Society for Testing and Materials, Philadelphia, PA, 1986.

17. ASTM Designation E264-82, "Standard Method for Determining Fast-Neutron Flux Density by Radioactivation of Nickel", in ASTM Standards, Section 12, American Society for Testing and Materials, Philadelphia, PA, 1986.

18. ASTM Designation E481-78, "Standard Method for Measuring Neutron-Flux Density by Radioactivation of Cobalt and Silver", in ASTM Standards, Section 12, American Society for Testing and Materials, Philadelphia, PA, 1986.

19. ASTM Designation E523-82, "Standard Method for Determining Fast-Neutron Flux Density by Radioactivation of Copper", in ASTM Standards, Section 12, American Society for Testing and Materials, Philadelphia, PA, 1986.

20. ASTM Designation E704-84, "Standard Method for Measuring Reaction Rates by Radioactivation of Uranium-238", in ASTM Standards, Section 12, American Society for Testing and Materials, Philadelphia, PA, 1986.

21. ASTM Designation E705-84, "Standard Method for Measuring Reaction Rates by Radioactivation of Neptunium-237", in ASTM Standards, Section 12, American Society for Testing and Materials, Philadelphia, PA, 1986.

22. ASTM Designation E1005-84, "Standard Method for Application and Analysis of Radiometric Monitors for Reactor Vessel Surveillance", in ASTM Standards, Section 12, American Society for Testing and Materials, Philadelphia, PA, 1986.

23. NUREG-0020, "Licensed Operating Reactors Status Summary Report", June 1981 through October 1988.

24. A. H. Fero, R. S. Bogg, W. T. Kaiser, WCAP-10814, "Analysis of Capsule U from the South Carolina Electric and Gas Company V. C. Summer Unit 1 Reactor Vessel Radiation Surveillance Program", June 1985.